

RESEARCH ARTICLE

Rewarding compounds identified from the medicinal plant *Rhodiola rosea*

Birgit Michels¹, Katrin Franke², Alicé Weiglein¹, Haider Sultani², Bertram Gerber^{1,3,4,*} and Ludger A. Wessjohann^{2,*}

ABSTRACT

Preparations of *Rhodiola rosea* root are widely used in traditional medicine. They can increase life span in worms and flies, and have various effects related to nervous system function in different animal species and humans. However, which of the compounds in *R. rosea* is mediating any one of these effects has remained unknown in most cases. Here, an analysis of the volatile and non-volatile low-molecular-weight constituents of *R. rosea* root samples was accompanied by an investigation of their behavioral impact on *Drosophila melanogaster* larvae. *Rhodiola rosea* root samples have an attractive smell and taste to the larvae, and exert a rewarding effect. This rewarding effect was also observed for *R. rosea* root extracts, and did not require activity of dopamine neurons that mediate known rewards such as sugar. Based on the chemical profiles of *R. rosea* root extracts and resultant fractions, a bioactivity-correlation analysis (AcorA) was performed to identify candidate rewarding compounds. This suggested positive correlations for – among related compounds – ferulic acid eicosyl ester (FAE-20) and β -sitosterol glucoside. A validation using these as pure compounds confirmed that the correlations were causal. Their rewarding effects can be observed even at low micromolar concentrations and thus at remarkably lower doses than for any known taste reward in the larva. We discuss whether similar rewarding effects, should they be observed in humans, would indicate a habit-forming or addictive potential.

KEY WORDS: *Drosophila melanogaster*, Learning, Memory, Olfaction, Reinforcement, Taste

INTRODUCTION

Rhodiola rosea L. (*Sedum roseum*) is a folk-medicine plant of the family Crassulaceae. In accordance with historical reports of the use of root material from this plant to treat headaches and ‘hysteria’ (Linnaeus, 1749), *R. rosea* products have been used for stress relief and the focusing of attention (Wiegant et al., 2009; Panossian et al., 2010). Contemporary scientific literature has reported increases in life span as a result of *R. rosea* food supplementation in the worm *Caenorhabditis elegans* and the fly *Drosophila melanogaster* (Jafari

et al., 2007; Wiegant et al., 2009; Gospodaryov et al., 2013; Arabit et al., 2018), as well as effects related to nervous system function. For example, food supplementation with *R. rosea* root material or extract enhances odor–reward associative memory in *Drosophila* larvae and can partially compensate for age-related memory decline in adult flies (Michels et al., 2018). In bees, acute food supplementation with *R. rosea* extract can enhance the acquisition and the consolidation of such associative memories (Michels et al., 2018). In neither case was behavior towards the odor or the reward affected. Memory-enhancing effects have also been reported in rodents and humans (Petkov et al., 1986; Panossian et al., 2010; Michels et al., 2018; but see Ishaque et al., 2012). However, whether one and the same chemical constituent of *R. rosea* mediates all these effects has remained unclear (for more details, please see Discussion). Indeed, identification of the respective bioactive compound(s) is critical not only for drug development but also for quality control during the production of *R. rosea* preparations, and for the dosage of *R. rosea* products. Possibly as a result of variation in their effect associated with variation in the concentration of the effective compounds, which cannot be determined as long as the effective compounds themselves have not been identified, the European Medicine Agency (EMA) and the National Institutes of Health of the USA (NIH) have issued skeptical reports (European Medicines Agency, 2012; <https://nccih.nih.gov/health/rhodiola>, accessed 27 July 2020). We have therefore endeavored to identify bioactive compounds from *R. rosea*, using for a bioassay the rewarding effect of its roots, which was discovered in the course of the present study.

So far, about 140 compounds have been detected in the roots of *R. rosea*, including phenylethanoids and phenylpropanoids, monoterpene alcohols, cyanogenic glycosides, flavonoids, proanthocyanidins and gallic acid derivatives (Panossian et al., 2010, and references therein). The observed effects have been considered to be mainly based on phenylethane and phenylpropane derivatives such as tyrosol and cinnamic alcohol and derived glycosides such as salidroside and rosavin. Thus, several commercial *R. rosea* preparations are standardized for their salidroside and rosavin content (Elameen et al., 2010). High rosavin levels seem to be characteristic for *R. rosea* and are used for differentiation from related species (Panossian et al., 2010). The main chemical classes of volatile compounds are monoterpene hydrocarbons, monoterpene alcohols and straight-chain aliphatic alcohols (Rohloff, 2002).

The starting point of the present study was the peculiar rose-like smell of ground *R. rosea* root material. Indeed, the common name of *R. rosea* in English is rose root. The monoterpene geraniol, its formate and acetate derivatives, as well as phenylethyl alcohol contribute to this rose-like odor (Rohloff, 2002). We report that for *Drosophila* larvae, a genetically tractable and placebo-clear model system, root material from *R. rosea* has an attractive smell as well as an attractive taste, and that *R. rosea* has a strong rewarding effect in these animals. We followed up on this latter observation and initiated a bioassay-

¹Leibniz Institute for Neurobiology (LIN), Department Genetics of Learning and Memory, 39118 Magdeburg, Germany. ²Leibniz Institute of Plant Biochemistry (IPB), Department of Bioorganic Chemistry, 06120 Halle (Saale), Germany. ³Otto von Guericke University, Institute of Biology, 39106 Magdeburg, Germany. ⁴Center for Behavioral Brain Sciences (CBBS), Otto von Guericke University, 39106 Magdeburg, Germany.

*Authors for correspondence (bertram.gerber@lin-magdeburg.de; wessjohann@ipb-halle.de)

© K.F., 0000-0003-3043-3571; B.G., 0000-0003-3003-0051; L.A.W., 0000-0003-2060-8235

guided fractionation approach supported by correlation analyses to identify the rewarding compound(s) in *R. rosea* (Degenhardt et al., 2014; Hielscher-Michael et al., 2016). We will briefly discuss whether these rewarding effects indicate a habit-forming or addictive potential, and weigh these effects against the recently reported memory-enhancing effect of both *R. rosea* and at least one of its compounds that are here identified as rewarding (Michels et al., 2018).

MATERIALS AND METHODS

Plant material

Crudely ground *R. rosea* root material was bought from Eveline24.de (Maardu, Estonia; Ch./ Lot: 17884). Voucher samples (QGB011; corresponding to the accession *Rhodiola*⁴) (Michels et al., 2018) are deposited at the IPB (Halle, Germany) and the LIN (Magdeburg, Germany). The traditional medicinal species *R. rosea* L. (Crassulaceae) is at present treated as a synonym of the accepted species *Sedum roseum* (L.) Scop. (accessed 1 January 2013: <http://www.theplantlist.org/>).

Metabolite analysis

General analytical methods

¹H nuclear magnetic resonance (NMR) and ¹³C NMR spectra were recorded in solutions on a Varian Mercury 400 spectrometer at 400 MHz and 101 MHz, respectively. Chemical shifts (δ) are reported in ppm and were referenced to TMS (¹H NMR) or to the solvent signal (¹³C NMR). Coupling patterns are designated as s(inglet), d(oublet), t(riplet), q(uartet), m(ultiplet), ps(eudo) and br(oad). The low-resolution electrospray (ESI) mass spectra were recorded on a SCIEX API-3200 instrument (Applied Biosystems, Concord, ON, Canada) combined with an HTC-XT autosampler. GC-ESI-MS measurements were obtained using a QP-2010 Ultra system (Shimadzu Corporation, Kyoto, Japan) equipped with a Phenomenex column (ZB-5MS, 30 m×0.25 μm) after trimethylsilylation of the compounds. For headspace gas chromatography mass spectrometry (GCMS) without derivatization, the following conditions were applied: incubation temperature 40°C, incubation time 30 min, syringe temperature 45°C, split injection (1:5), detected mass-to-charge ratio (*m/z*) 40–500, injector port temperature 220°C, source temperature 220°C, interface temperature 300°C, carrier gas helium, column flow 1.02 ml min^{−1}, column temperature program: 40°C for 1 min, then raised to 300°C at a rate of 10°C min^{−1} and held on 300°C for 5 min. Before measurement, the sample was wetted with water. Compounds were identified by comparing their electron ionization-mass spectrometry (EI-MS) spectra with the NIST 08 or NIST 11 database. The relative abundance of components was calculated based on the peak areas of the total ion chromatogram. Ultra-high performance liquid chromatography-high-resolution mass spectrometry (UHPLC-HRMS) measurements were

performed as previously described (Coors et al., 2019). TLC was performed on silica gel 60 *F*₂₅₄ plates (Merck). Spots were visualized using UV light and vanillin-H₂SO₄ detection reagent. For preparative column chromatography (CC), silica gel 60 (63–200 μm and 40–63 μm) was used.

ESI-FTICR-MS

High-resolution electrospray ionization (ESI) mass spectra were obtained from a Bruker Apex III Fourier transform ion cyclotron resonance (FTICR) mass spectrometer (Bruker Daltonics, Billerica, MA, USA) equipped with an Infinity™ cell, a 7.0 T superconducting magnet (Bruker, Karlsruhe, Germany), a radio-frequency-only hexapole ion guide and an external APOLLO electrospray ion source (Agilent, off-axis spray, voltages: negative ion mode: endplate, 3700 V; capillary, 4200 V; capillary exit, −100 V; skimmer 1, −15.0 V; skimmer 2, −6.0 V; offset −3.75 V; positive ion mode: endplate, −3700 V; capillary, −4.200 V; capillary exit, 100 V; skimmer 1, 15.0 V; skimmer 2, 12.0 V; offset 3.75 V). Nitrogen was used as a drying gas at 150°C. The sample solutions were introduced continuously via a syringe pump with a flow rate of 120 μl h^{−1}. The instrument was externally calibrated using the ES tuning mix (Agilent G2422A). The data were acquired with 512 k data points and zero-filled to 2048 k by averaging 12 scans (ion accumulation: 1 s). The mass spectra were evaluated using the Bruker software XMASS 7.0.8.

Activity correlation analysis (AcorA)

To relate the metabolite profiles obtained by direct-infusion ESI-FTICR-MS to the rewarding activity of the respective plant-derived materials, reverse metabolomics with the AcorA algorithm was used (Degenhardt et al., 2014; Hielscher-Michael et al., 2016). In brief, from the fractions resulting from liquid–liquid partitioning of the *R. rosea* crude extract and the sub-fractions E1–E5 and H1–H4, 1 ml of a solution in methanol (10 mg ml^{−1}) was purified using a Chromabond® RP18 SPE cartridge (Macherey-Nagel). The resulting samples were adjusted to a concentration of 1 mg ml^{−1} and 100 μl of the solution was diluted with 500 μl methanol, centrifuged and then subjected to triplicate high-resolution electrospray ionization mass spectrometry (HRESIMS) measurements. The ESI-FTICR-MS files were converted to the mzData file format. After peak-picking and aligning the data from the positive ionization mode using the R package XCMS (Smith et al., 2006), 936 different *m/z* features were detected. To determine the correlation between the rewarding activity and the mass signal intensities, the Spearman rank correlation coefficient was calculated after performing a permutation test with 500 repeats. This AcorA resulted in the identification of 51 positively correlating features (Table 1; Table S1). The elemental composition of the correlating features was calculated based on the ESI-FTICR-MS

Table 1. Highest-ranked high-resolution electrospray ionization mass spectrometry (HRESIMS) signals (*m/z* features) correlating with the rewarding effect of *Rhodiola* fractions

Rank no.	FTICR-HR <i>m/z</i>	Spearman coefficient	Formula	MW	RDB	Calculated	Proposal
1	485.36057	0.764	C ₂₉ H ₅₀ O ₄ Na ⁺	462	4.5	485.36013	–
2	365.26635	0.664	C ₂₀ H ₃₈ O ₄ Na ⁺	342	1.5	365.26623	Oxygenated fatty acid
3	497.36086	0.662	C ₃₀ H ₅₀ O ₄ Na ⁺	474	5.5	497.36013	Ferulic acid eicosyl ester (FAE-20)
4	629.40341	0.624	C ₃₅ H ₅₈ O ₈ Na ⁺	606	6.5	629.40239	Triterpene glycoside
5	393.29800	0.605	C ₂₂ H ₄₂ O ₄ Na ⁺	370	1.5	393.29753	Oxygenated fatty acid
6	639.49637	0.605	C ₃₉ H ₆₈ O ₅ Na ⁺	616	5.5	639.49590	Diglyceride
7	319.22432	0.595	C ₁₈ H ₃₂ O ₃ Na ⁺	296	2.5	319.22437	Oxygenated fatty acid
8	335.21937	0.593	C ₁₈ H ₃₂ O ₄ Na ⁺	312	2.5	335.21928	Oxygenated fatty acid
9	613.40841	0.588	C ₃₅ H ₅₈ O ₇ Na ⁺	590	6.5	613.40747	Triterpene glycoside
10	359.14678	0.571	C ₁₈ H ₂₄ O ₆ Na ⁺	336	6.5	359.14651	–

FTICR-HR, high-resolution Fourier transform ion cyclotron resonance mass spectrometry. A full list of correlating features is given in Table S1.

results. The ESI-FTICR-MS data from the negative ionization mode could not be correlated because of an unsuccessful R-data conversion and the limitations of the Bruker software.

Bioactivity-guided fractionation and isolation

Finely chopped *R. rosea* root (1.565 kg) was exhaustively extracted with 80% aqueous un-denatured ethanol (3×6 l) at room temperature. The extracts were combined, filtered and the organic solvent evaporated under reduced pressure until the aqueous residue remained. This crude extract was successively partitioned with 3×500 ml *n*-heptane, ethyl acetate and *n*-butanol, resulting, after removal of the solvents, in fractions of different polarity: *n*-heptane (Rho_{heptane} , 8.72 g), ethyl acetate ($Rho_{\text{ethyl acetate}}$, 25.66 g), *n*-butanol (Rho_{butanol} , 92.42 g) and water (Rho_{water} , 312.01 g). Following assessment of their influence as a reward in associative learning in larval *Drosophila*, the active fractions were further separated according to polarity using silica gel column chromatography.

A 3.40 g sample of the $Rho_{\text{ethyl acetate}}$ fraction was sub-fractionated on a short column, eluting with a gradient system: 250 ml *n*-hexane, 300 ml chloroform (combined E1, 0.38 g), 300 ml ethyl acetate (E2, 1.40 g), 200 ml ethyl acetate/methanol (8:2; E3, 0.51 g), 300 ml methanol (E4, 0.34 mg) and 300 ml methanol containing 2 ml 2 mol l⁻¹ HCl (E5, 1.15 g).

A part of the active *n*-heptane fraction (4.90 g Rho_{heptane}) was sub-fractionated using *n*-heptane (H1, 1.22 g), CHCl₃ (H2, 0.66 g), ethyl acetate (H3, 2.06 g) and methanol (H4, 0.60 g), 500 ml in each case, as eluting solvents to give the respective sub-fractions.

The resulting sub-fractions E1–E5 and H1–H4 were then assayed for their activity as a reward as described below.

Isolation and structure elucidation

The most active fractions and compounds associated with the best-correlating peaks from AcorA (see above) were separated and characterized as detailed in the following.

β-Sitosterol-β-D-glucoside

The most active sub-fraction (E5) was further separated by column chromatography on silica gel, eluting with a chloroform/methanol gradient to obtain β-sitosterol-β-D-glucoside (32.7 mg) as the major constituent.

β-Sitosterol-β-D-glucoside (BSSG): ¹H NMR (400 MHz, DMSO) δ [ppm]: 5.329 (brs, 1H, H-6); 4.220 (d, *J*=7.9 Hz, 1H, H-1'); 0.957 (s, 3H, H-19); 0.902 (d, *J*=6.6 Hz, 3H, H-21); 0.651 (s, 3H, H-18). ¹³C NMR (100 MHz, DMSO) δ [ppm]: 140.5 (C5), 121.2 (C6), 100.8 (C1'), 77.0 (C3), 76.7 (C3'), 76.7 (C5'), 73.4 (C2'), 70.0 (C4'), 61.0 (C6'), 56.2 (C14), 55.4 (C17), 49.6 (C9), 45.2 (C24), 41.9 (C13), 39.3 (C12, under DMSO signal), 38.3 (C4), 36.8 (C1), 36.2 (C10), 35.5 (C20), 33.4 (C22), 31.44 (C8), 31.4 (C7), 29.3 (C2), 28.7 (C25), 27.8 (C16), 25.5 (C23), 23.9 (C15), 22.6 (C28), 20.6 (C11), 19.7 (C27), 19.1 (C19), 18.9 (C26), 18.6 (C21), 11.8 (C29), 11.7 (C18). The NMR data are in accordance with Faizi et al. (2001).

Ferulic acid eicosyl ester and further E5 constituents

Also from the E5 sub-fraction, ferulic acid eicosyl ester was isolated, ESI-MS guided by the occurrence of the ion at *m/z* 497 [M+Na]⁺ of the correlating feature 3 (Table 1) in positive ionization mode, as previously described (Michels et al., 2018). Therefore, an aliquot of the ethyl acetate extract ($Rho_{\text{ethyl acetate}}$, 7.8 g) was fractionated in analogy to the above-described sub-fractionation procedure on a short silica gel column, eluting with 400 ml chloroform (3.79 g), 300 ml ethyl acetate (2.50 g) and 200 ml methanol (1.30 g). The fraction eluted with

chloroform was subjected to repeated column chromatography on silica gel using a gradient system (*n*-hexane:CHCl₃ 8:2 gradient to 0:1, followed by ethyl acetate and methanol), followed by column chromatography with CHCl₃ affording 15.5 mg ferulic acid eicosyl ester in a 3:1 mixture as *trans* and *cis* (interconvertible) diastereomers, 13.3 mg fatty alcohol and 2.2 mg stigmast-4-en-3-one.

Ferulic acid eicosyl ester (FAE-20): ESI-MS, 473.3647 [M-H]⁻ calculated for C₃₀H₄₉O₄⁻ 473.3636 accompanied by homologs bearing a C₁₈ or C₂₂ fatty alcohol chain: 445 [M-H]⁻ in accordance with C₂₈H₄₅O₄⁻ (FAE-18); and 501.3959 [M-H]⁻ calc. for C₃₂H₅₃O₄⁻ 501.3949 (FAE-22). ¹H NMR (400 MHz, CDCl₃) δ [ppm]: *trans*: 7.608 (d, *J*=16 Hz, 1H, H-7); 7.075 (dd, *J*=8, 2, 2H, H-6); 7.037 (d, *J*=2 Hz, 1H, H-2); 6.913 (d, *J*=8 Hz, 1H, H-5); 6.291 (d, *J*=16 Hz, 1H, H-8); 5.993 (s, 1H, OH); 4.187 (t, *J*=7 Hz, 2H, H1'); 3.930 (s, 3H, OMe); 1.638 (m, 2H, H-2'); 1.45–1.21 (m, 10H); 0.879 (t, *J*=7 Hz, 3H, Me-20'). *cis*: 7.756 (d, *J*=2 Hz, 1H, H-2); 7.103 (dd, *J*=8, 2, 1H, H-6); 6.878 (d, *J*=8, 1H, H-5); 6.795 (d, *J*=12.7 Hz, 1H, H-7); 5.948 (brs, 1H, OH); 5.815 (d, *J*=12.5 Hz, 1H, H-8); 4.117 (t, *J*=7 Hz, 2H, H-1'); 3.930 (s, 3H, OMe). ¹³C NMR (100 MHz, CDCl₃) δ [ppm]: *trans*: 167.4 (C9); 147.9 (C3); 146.7 (C4); 144.6 (C7); 127.0 (C1); 123.0 (C6); 115.6 (C8); 114.7 (C5); 109.3 (C2); 64.6 (C1'); 55.9 (OMe); 31.9 (C2'); 29.7; 29.63; 29.58; 29.5; 29.34; 29.28; 28.8; 26.0; 22.7 (C3'-C19'); 14.1 (Me). *cis*: 166.7 (C9); 147.0 (C4); 143.7 (C7); 127.0 (C1); 125.5 (C6); 116.9 (C5); 113.8 (C8); 112.7 (C2); 64.4 (C1'); 55.9 (OMe). The NMR data are in agreement with Hennig et al. (2011) and Baldé et al. (1991).

Fatty alcohols: gas chromatography electron ionization mass spectrometry (GC-EI-MS): octadecanol 1.6%, nonadecanol 0.4%, eicosanol 69.2%, heneicosol 1.3%, docosanol 27.0%, tetracosanol 0.5%. ¹H NMR (400 MHz, CDCl₃) δ [ppm]: 3.639 (t, *J*=7.0 Hz, 2H); 1.566 (m); 1.360–1.255 (m); 0.880 (t, *J*=7.0, 3H).

Stigmast-4-en-3-one: ESI-MS, *m/z*: 413 [M+H]⁺, 435 [M+Na]⁺, 825 [2M+H]⁺. ¹H NMR (400 MHz, CDCl₃) δ [ppm]: 5.722 (s, 1H, H-4); 1.181 (s, 3H, H-19); 0.926–0.782 (m, H-21, H-26, H-27, H-29); 0.710 (s, 3H, H-18).

Linoleic and other fatty acids

A part of the sub-fraction H3 was purified by column chromatography on silica gel, eluting with CHCl₃ (400 ml), followed by CHCl₃:methanol 9:1 (300 ml) and methanol (300 ml), to obtain an unsaturated fatty acid fraction (FA_{isolated}) consisting mainly of linoleic acid (51.2 mg).

Linoleic acid: ESI-MS, *m/z*: 279 [M-H]⁻, 303 [M+Na]⁺. ¹H NMR (400 MHz, CDCl₃) δ [ppm]: 5.417–5.301 (m, -CH=CH-); 2.823–2.756 (m, =CH-CH₂-CH=); 2.347 (t, -CH₂-COOH); 2.098–1.989 (m, -CH₂-CH=); 1.651–1.597 (m, -CH₂-CH₂-COOH); 1.393–1.256 (m, -CH₂-); 0.890 (t, CH₃).

Syntheses

β-Sitosterol-β-D-glucoside and *trans*-ferulic acid eicosyl ester were synthesized as previously described (Michels et al., 2018).

Biological assays

Flies and fly keeping

Wild-type *D. melanogaster* larvae were used throughout, unless mentioned otherwise. They were of the Canton-Special (CS) strain and aged 5 days after egg laying, still in their feeding stage. Animals were kept in mass culture, maintained at 25°C, 60–70% relative humidity and a 12 h:12 h light:dark cycle.

The anosmic *Orco*¹ mutant strain (Bloomington Stock Center no. 23129) carries a loss-of-function allele of the *Orco* gene and has been described previously (Larsson et al., 2004; Vosshall and Hansson, 2011). The mushroom body driver strain *OK107-Gal4* (Connolly et al., 1996), the split-Gal4 strains *APL-Gal4* (SS01671), *DAN-h1-Gal4* (SS01696) (Saumweber et al., 2018) and *DAN-h1, DAN-il, DAN-j1, DAN-k1-Gal4* (with *DAN-j1* included only stochastically; SS01948) (Eschbach et al., 2020) were crossed to *UAS-Kir2.1::GFP* (*Kir*^{GFP}) (Saumweber et al., 2018) as the effector for neuronal silencing in the experimental genotypes. To obtain the driver controls, the Gal4 driver strains were crossed to the CS wild-type strain, as this was the genetic background of the effector strain that was omitted from the cross (Saumweber et al., 2018). As effector controls, a strain homozygous for both the attP40 and attP2 landing sites, but without a Gal4 inserted, was the genetic background of the split-Gal4 driver strains ('empty' Gal4; Pfeiffer et al., 2010) and was therefore used for generating the effector control when the experimental genotypes featured a split-Gal4 driver element; for the experiment featuring *OK107-Gal4*, the genetic background of the driver strain was *w¹¹¹⁸* and this strain was used for generating the effector control; in both cases, the crossings yielding the effector control were carried out with *UAS-Kir2.1::GFP*. Experimenters were blind to genotype.

Immunohistochemistry

To verify effector expression from *UAS-Kir2.1::GFP*, larval brains of experimental genotypes were dissected in Ringer solution and fixed in 4% paraformaldehyde dissolved in PBS for 30 min. After three washes (each 10 min) in PBST, the brains were treated in blocking solution containing 3% normal goat serum (Dianova) in PBS for 2 h. Tissue was then incubated overnight with the primary antibodies rabbit anti-GFP (1:1000; Invitrogen A11122) and mouse anti-FASII (1:50; DSHB). Six washing steps in PBS (each 10 min) were followed by incubation with Alexa Fluor 488 goat anti-rabbit (1:200; Invitrogen A11034) and Cy3 donkey anti-mouse (1:200; Jackson ImmunoResearch Laboratories 715-165-150) as secondary antibodies. After final washing steps with PBS, samples were mounted in Vectashield (Linaris) and scanned under a confocal microscope. Projections of the stacks were accomplished with Fiji ImageJ software.

Behavioral experiments

For the behavioral experiments, the *R. rosea* root was finely ground using a Precellys 24 homogeniser (VWR, Erlangen, Germany). For simplicity, the resulting root powder will be called *Rhodiola* throughout the paper. For the behavioral experiments, Petri dishes (Sarstedt, Nümbrecht, Germany) with an inner diameter of 60 mm were filled with 1% agarose (electrophoresis grade; Roth, Karlsruhe, Germany), allowed to solidify, covered with their lids, and then left untreated at 4°C until the next day. To serve as a potential reinforcer, these could be supplemented with 0.1, 1.0 or 10.0 mg ml⁻¹ *Rhodiola* mixed into a 1% agarose solution shortly after boiling the agarose solution.

All the behavioral experiments were performed under natural light at 22–25°C. Animals were randomly collected from the food vial by removing a spoonful of food medium containing larvae and were transferred to a tap-water droplet on a plain plastic Petri dish. From this droplet, cohorts of 15 animals were collected, briefly washed in tap water and transferred for the respective experiment.

Testing olfactory and gustatory preference for *Rhodiola*

For the olfactory preference tests, we added *Rhodiola* to custom-made Teflon containers of 5 mm inner diameter such that the

bottom of the containers was covered. These containers, which are available from the authors upon request, were covered with lids perforated by 7 holes of 0.5 mm diameter each and placed to one side of a 60 mm Petri dish filled with agarose as substrate. The other side featured empty containers. Cohorts of 15 experimentally naive larvae were placed in the middle; in this setup, the larvae could thus smell, but not taste, the *Rhodiola* in the containers. After 3 min, the number of larvae (*n*) was determined on the *Rhodiola* side, on a 7 mm neutral zone, or on the side with the empty odor containers. Then the olfactory preference score was calculated as:

$$\text{Pref}_{\text{odor}} = (n_{\text{Rhodiola}} - n_{\text{empty}}) / n_{\text{total}} \quad (1)$$

Thus, scores ranged between −1 and 1: positive $\text{Pref}_{\text{odor}}$ scores indicate approach towards the smell of *Rhodiola*, whereas negative scores indicate avoidance of it.

For the gustatory preference tests, cohorts of 15 larvae were placed in the middle of a split 60 mm diameter Petri dish. One half of the dish had an agarose substrate with added *Rhodiola* (10 mg ml⁻¹), while the other half had only agarose. Thus, in this setup the larvae could both taste and smell *Rhodiola*. After 3 min, the number of larvae on either side was determined and a preference score was calculated as:

$$\text{Pref}_{\text{odor/taste}} = (n_{\text{Rhodiola}} - n_{\text{agarose}}) / n_{\text{total}} \quad (2)$$

In this case too, scores ranged between −1 and 1: positive Pref scores reveal attraction to *Rhodiola*, whereas negative scores indicate aversion.

Testing the reward capacity of *Rhodiola*

The odor–reward associative learning experiments follow the procedures introduced by Scherer et al. (2003) and Neuser et al. (2005) for the association of odor with fructose as the reward in the two-group, one-odor version introduced by Saumweber et al. (2011) (for a detailed manual, see Michels et al., 2017) – with the modification that instead of fructose, *Rhodiola* was used. In brief, an odor was presented to separate groups of animals, either paired or unpaired with *Rhodiola* during training, followed by an odor preference test. A higher test preference for the odor after paired versus unpaired training indicates appetitive associative memory; that is, it indicates that *Rhodiola* was effective as a reward.

Odor was applied by adding 10 µl of *n*-amyl acetate (AM; CAS: 628-63-7; purity: 98.5%, diluted 1:50 in paraffin oil; Merck, Darmstadt, Germany) to the Teflon containers described above. These were placed into Petri dishes with either plain agarose as the substrate or agarose supplemented with *Rhodiola* at the amounts mentioned in Results.

For the learning experiments, the regular lids of the Petri dishes were replaced by lids perforated in the center by 15 holes of 1 mm diameter to improve aeration. Then, a cohort of 15 larvae was placed into a Petri dish featuring, for example, AM as the odor and *Rhodiola* as the reward. The Petri dish was closed with its lid and the larvae were allowed to move freely for 5 min. Then the larvae were transferred to a Petri dish with an empty odor container (Em) and agarose as the substrate. Such paired training (AM+/Em) was repeated two more times. In half of the cases, the sequence of training trials was as indicated in this example; in the other half it was the reverse (Em/AM+). Unpaired training consisted of separate presentations of odor and *Rhodiola* (AM/Em+ or when using the reverse sequence of trials Em+/AM). After either paired or unpaired training, the larvae were tested for their odor preference by allowing them to choose between two sides of a test Petri dish, one with an AM-filled odor container and the other with an empty odor container

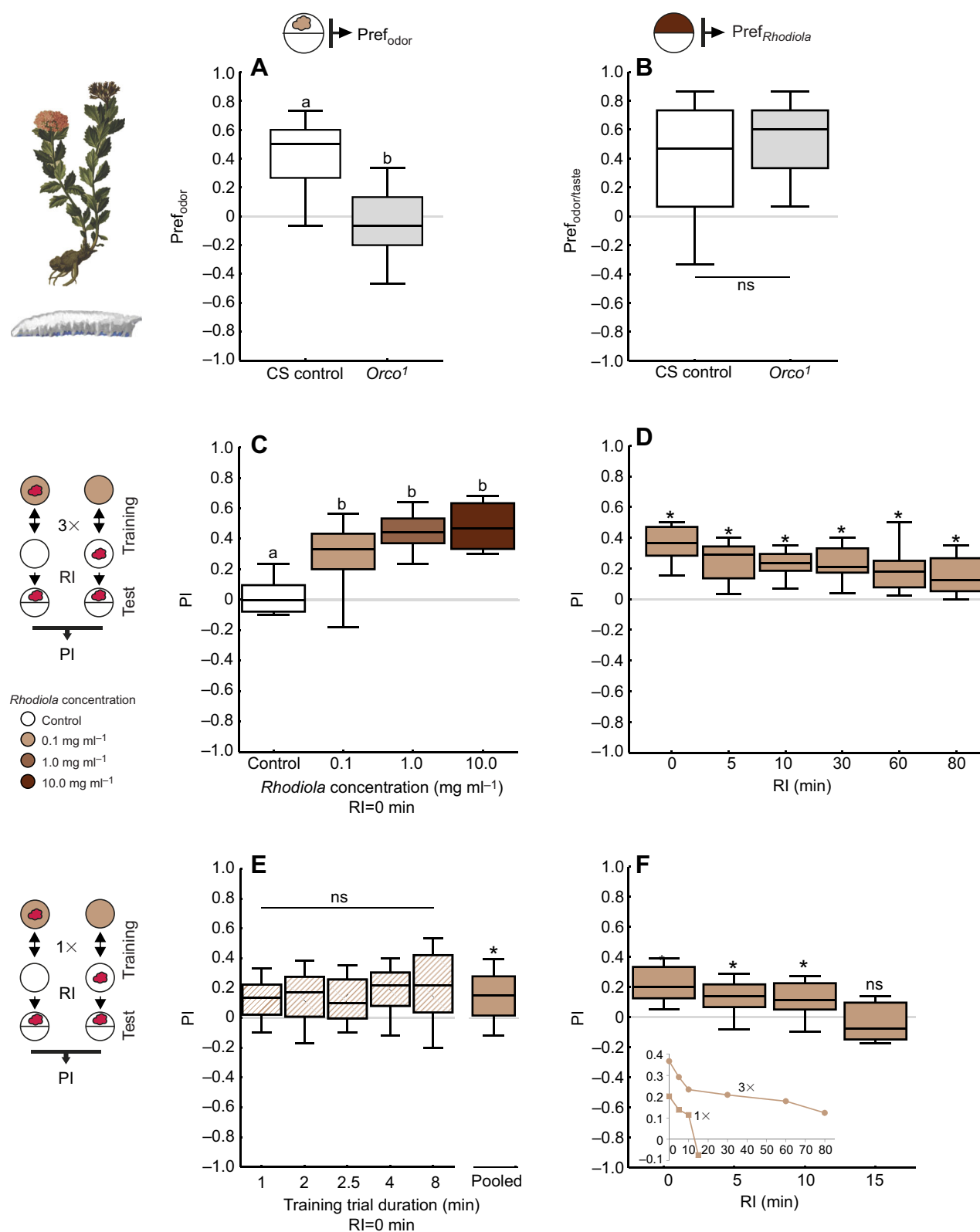


Fig. 1. See next page for legend.

(the test Petri dish featured agarose alone as the substrate). After 3 min, the number of animals on the odor side and no-odor side and in the neutral zone (5 mm) was counted and the odor preference determined, with due adjustments, as in Eqn 1.

To determine whether odor preference differed depending on the training regimen, the preference data from paired-trained and unpaired-trained cohorts of animals were taken and, for pairs of data gathered in parallel, the performance index (PI) was

Fig. 1. *Rhodiola* root is attractive and rewarding to larval *Drosophila*.

(A,B) Drawings of *Rhodiola* [modified from <https://www.flickr.com/photos/internetarchivebookimages/20317664056/> – original drawing from Atlas der Alpenflora (1882)] and a *Drosophila* larva are shown on the left. (A) The sketch at the top shows the odor preference task (brown cloud: odor from ground *Rhodiola* root). Preference scores indicate that wild-type Canton-S (CS) control larvae showed attraction to the odor of *Rhodiola*, whereas attraction was abolished in anosmic mutant larvae [*Orco*¹; *U*-test, $P < 0.05$, $U = 36.0$, $N = 18$, 18; one-sample sign test (OSS), CS: $P < 0.05/2$, *Orco*¹: $P > 0.05/2$]. (B) The odor/taste preference task is shown at the top (brown: ground *Rhodiola* root 10 mg ml⁻¹ added to agarose, white: plain agarose). Preference scores for the anosmic *Orco*¹ mutant larvae did not significantly differ from those of wild-type CS control larvae in a combined smell/taste preference task (*U*-test, $P > 0.05$, $U = 198.0$, $N = 35$, 14). (C,D) The use of ground *Rhodiola* root as a reward in a Pavlovian conditioning experiment is sketched on the left (red cloud: *n*-amyl acetate odor, brown circles: Petri dishes filled with agarose supplemented with the indicated concentrations of ground *Rhodiola* root, white circles: plain agarose Petri dishes). (C) In separate groups of wild-type larvae, the odor was presented either paired or unpaired with *Rhodiola* as a reward. After three cycles of training, the preference for the odor was measured, and associative memory was quantified as the performance index (PI), reflecting the difference in preference between paired-trained and unpaired-trained groups of larvae. At all three doses tested, the memory scores significantly differed from those of the control, for which *Rhodiola* was omitted from the experiment (*H*-test, $P < 0.05$, $H = 33.9$, d.f.=3, $N = 12$, 33, 33, 33; *U*-tests, 0.1 mg ml⁻¹ *Rhodiola*: $P < 0.05/3$, $U = 100.0$; 1.0 mg ml⁻¹ *Rhodiola*: $P < 0.05/3$, $U = 19.0$; 10.0 mg ml⁻¹ *Rhodiola*: $P < 0.05/3$, $U = 14.0$). (D) Larvae trained with the lowest dose of *Rhodiola* showed associative memory that remained significantly different from chance level (zero) until 80 min after training (*H*-test, $P < 0.05$, $H = 22.7$, d.f.=5, $N = 21$, 21, 22, 17, 17, 22; OSS tests, $P < 0.05/6$ for all tested time points). RI, retention interval. (E,F) Larvae underwent the learning paradigm shown in C but with only one cycle of training and with 0.1 mg ml⁻¹ *Rho*_{extract} (brown) as the reward, as shown on the left (for further parametric deviations, see Materials and Methods). (E) Memory scores of larvae trained with different training trial durations did not differ from each other (*H*-test, $P > 0.05$, $H = 4.2$, d.f.=4, $N = 28$ for each group). The PI of all groups pooled was significantly different from zero (right-most boxplot, OSS test, $P < 0.05$, $N = 140$). (F) The memory scores of larvae trained with a 4 min trial duration remained detectable until 10 min after training (*H*-test, $P < 0.05$, $H = 21.1$, d.f.=3, $N = 20$ for each group; OSS tests, 0, 5 and 10 min: $P < 0.05/4$, 15 min: $P > 0.05/4$), indicating less stable memory than after three training cycles (D). The inset shows the median values from D (3×) and F (1×). * $P < 0.05$; ns: $P > 0.05$. 'b' above the boxplot indicates a significant difference from wild-type CS control or control (these are labeled with 'a') in *U*-tests; in C, these were Bonferroni corrected ($P < 0.05/3$). Box plots represent the median as the middle line, 25% and 75% quantiles as box boundaries, and 10% and 90% quantiles as whiskers. Data are documented in Table S3. Preference scores underlying the PIs are documented in Fig. S4.

calculated as:

$$PI = (\text{Pref}_{\text{AM+}/\text{Em}} - \text{Pref}_{\text{AM}/\text{Em+}})/2. \quad (3)$$

Again, scores ranged between -1 and 1. Given that larvae of both groups were equated for handling and stimulus exposure and thus for the effects of non-associative learning, positive PI scores indicate appetitive associative memory, i.e. a rewarding effect exerted by *Rhodiola*. Negative scores indicate aversive associative memory, i.e. a punishing effect exerted by *Rhodiola*.

The Petri dishes were coded such that experimenters were blind with respect to whether the Petri dishes featured *Rhodiola* or not. This was decoded only after the experiment.

For the control group, the procedure was identical to the above (including mock-codes of the Petri dishes), except that *Rhodiola* was omitted. Data for the *Rhodiola* and the control groups were gathered alternately. This is essential for meaningful statistical comparisons, given the variability of memory scores in the larvae (and indeed in *Drosophila* and insects in general).

The one-trial version of the learning paradigm followed the same principle, without repeating the training cycle. To match our procedures to a recent report of one-trial learning with various other tastant reinforcers (Weiglein et al., 2019), these experiments featured 30 larvae, Petri dishes of 90 mm diameter, AM at a 1:20 dilution as the odor, and training trials that lasted 4 min, unless mentioned otherwise.

Testing the reward capacity of further substances

Exactly the same learning protocols as described above were used whenever either fructose (2 mol l⁻¹; purity: 99%; Roth, Karlsruhe, Germany) or *Rhodiola*-related candidate rewarding substances were used (e.g. those with a positive AcorA value). If these substances were added to the agarose in dissolved form, using an appropriate solvent, we also included solvent groups in our experiments. In other words, the only difference between the experimental groups, trained with the candidate rewarding compound, and the corresponding solvent group was whether or not the candidate compound was present. Except for the fractions (*Rho*_{heptane}, *Rho*_{butanol}, *Rho*_{ethylacetate}, *Rho*_{water}), all substances were dissolved in 100% ethanol. The candidate substances tested for their reward capacity, at the concentrations mentioned in Results and in the figures, were as follows (for details of how these were obtained, please see sections above): *Rhodiola* crude extract (*Rho*_{extract}); fractions of *Rho*_{extract} (*Rho*_{water}, *Rho*_{butanol}, *Rho*_{ethylacetate}, *Rho*_{heptane}) dissolved in water (*Rho*_{water}), 50% aqueous ethanol (*Rho*_{butanol}) or 80% aqueous ethanol (*Rho*_{ethyl acetate} and *Rho*_{heptane}), with the respective solvents being used for the solvent groups; sub-fractions of the ethyl acetate (E1-5) and the heptane fractions (H1-4); isolated and synthesized β-sitosterol-β-D-glucoside (BSSG_{isolated} and BSSG_{synthesized}); isolated and synthesized ferulic acid ester (FAE-20_{isolated} and FAE-20_{synthesized}); isolated fatty acid fraction (FA_{isolated}); *trans*-ferulic acid (purity 99%, Aldrich, Darmstadt, Germany); 1-eicosanol (purity 96%, Alfa Aesar, Karlsruhe, Germany); and stigmasterol (purity 95%, ACROS Organics, Morris Plains, NJ, USA). Experimenters were blind to the substance used.

Statistical analyses of behavioral data

Statistical analyses of behavioral data were performed with Statistica (version 8.0, StatSoft, Inc., Tulsa, OK, USA) on a PC. In a conservative approach, non-parametric tests were used throughout. For comparisons with chance levels (i.e. with zero), one-sample sign tests (OSS) were applied (<http://www.R-project.org/>) and for multiple-group comparisons, Kruskal–Wallis (*H*) tests were used. In the case of significance, follow-up pairwise comparisons using Mann–Whitney *U*-tests were conducted. The significance level used was 5%, and maintained at that level in the case of multiple comparisons within one experiment by using a Bonferroni correction ($P < 0.05$ divided by the respective number of pairwise tests). Data are displayed as box plots representing the median as the middle line, 25% and 75% quantiles as box boundaries, and 10% and 90% quantiles as whiskers.

All experiments and analyses comply with applicable ethical regulations and law. The data underlying the presented figures and used for statistical analyses are documented in the analytical and behavior data files (Table S2 and Table S3). Assuming that effect sizes for the materials used as rewards in the present study would be equal to or moderately less than those in previous studies from our laboratory using 'canonical' rewards, sample sizes were limited to a range equal to or slightly higher than in our previous publications. The same applies for the olfactory and gustatory preference assays.

RESULTS

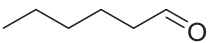
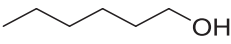
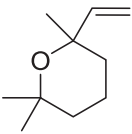
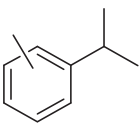
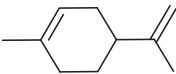
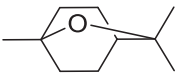
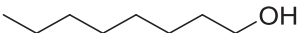
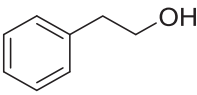
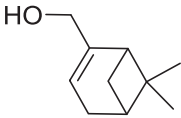
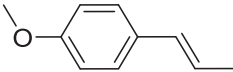
Smell and taste of *Rhodiola* are attractive to larval*Drosophila*

The first time we used freshly ground, dried *R. rosea* root material, our attention was caught by a pleasant, mild, fruity, rose-like smell combined with a peculiar note reminiscent of rubber. This prompted us to ask whether our experimental animals too might find *Rhodiola* to have an attractive smell. Wild-type CS larvae showed attraction to *Rhodiola* in an olfactory preference test; this attraction was abolished in mutant larvae carrying a loss-of-function mutation in the *Orco* gene (Fig. 1A). This gene codes for an olfactory co-receptor required for sensory function in all known larval

olfactory sensory neurons, its loss rendering the animals unresponsive to odors but leaving taste processing unaffected. We conclude that the net effect of the volatile compounds from *Rhodiola* (Table 2) is attractive to larval *Drosophila*, and requires *Orco* function.

We found *Rhodiola* to have a delayed yet strong, unpleasant and ‘dry’, astringent, bitter taste, so we wondered whether *Rhodiola* might have an aversive taste to the larvae, too. This was not the case. Rather, wild-type larvae showed attraction in a combined odor/taste preference test; the fact that the anosmic *Orco*¹ mutant larvae likewise showed such attraction (Fig. 1B) suggests that in these mutants the taste of *Rhodiola* is attractive.

Table 2. Volatile odor compounds from *Rhodiola* root detected by headspace gas chromatography mass spectrometry (GCMS)

Rt (min)	Structure	Molecular weight/formula	Compound	Relative composition (%)
4.34		100/C ₆ H ₁₂ O	Hexanal	19.1
5.43		102/C ₆ H ₁₄ O	Hexanol	4.2
7.15		154/C ₁₀ H ₁₈ O	Linalyl oxide	10.8
8.02		134/C ₁₀ H ₁₄	Cymene (o, p or m)	12.4
8.10		136/C ₁₀ H ₁₆	Limonene	7.3
8.16		154/C ₁₀ H ₁₈ O	Eucalyptol	2.8
8.71		130/C ₈ H ₁₈ O	n-Octanol	7.6
9.45		122/C ₈ H ₁₀ O	Phenylethanol	14.2
10.77		152/C ₁₀ H ₁₆ O	Myrtenol	14.3
12.04		148/C ₁₀ H ₁₂ O	Estragol	6.7

Rt, retention time.

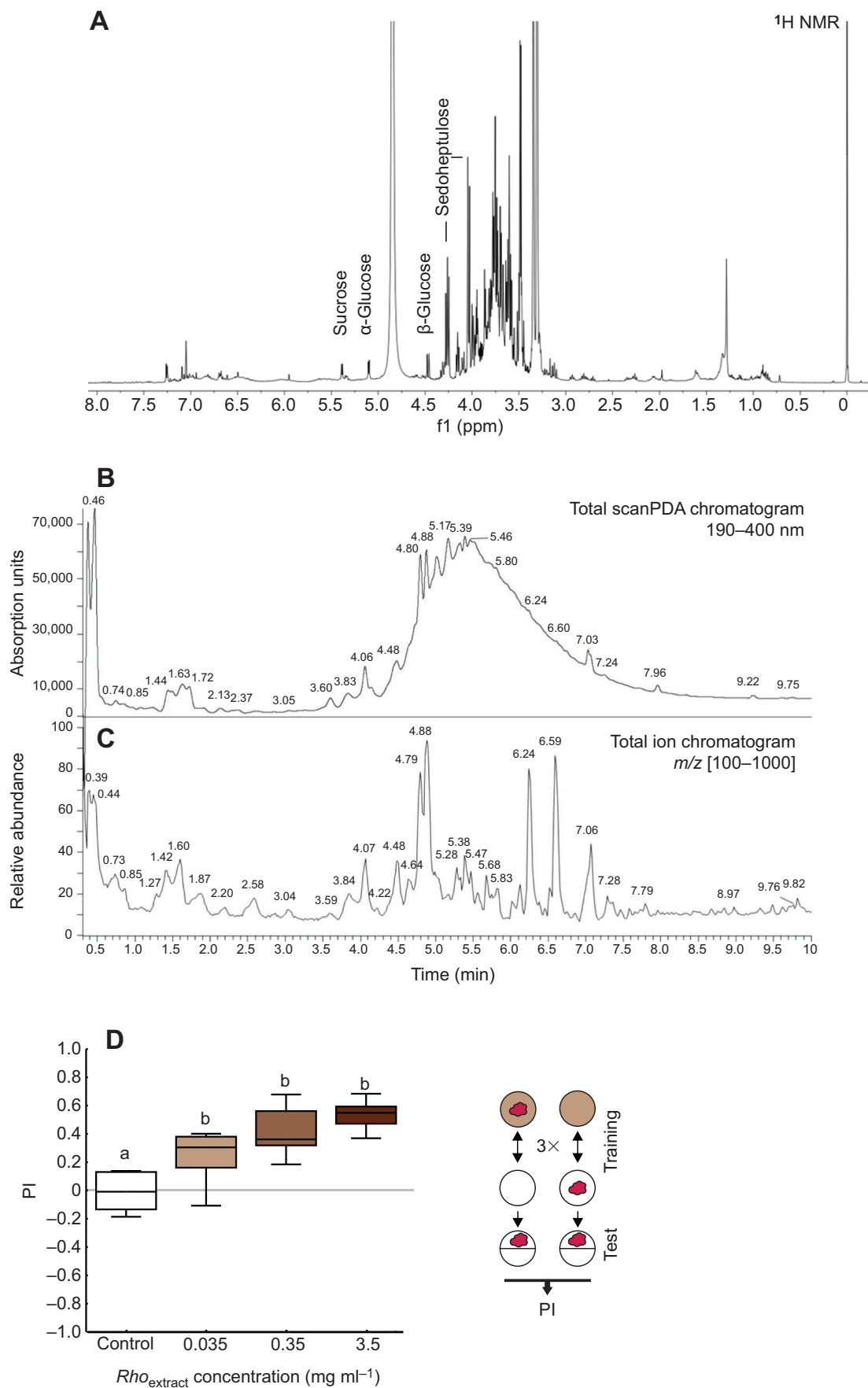


Fig. 2. See next page for legend.

Fig. 2. Chemical properties and rewarding effect of the *Rhodiola* crude extract (Rho_{extract}). (A) Documentation of the ^1H NMR (measured in deuterated methanol), (B) ultra-high performance liquid chromatography-photodiode array (UHPLC-PDA) and (C) high-resolution mass spectrometry (HRMS) fingerprints of the Rho_{extract} (see Table 3 for compound annotation). f1, frequency coordinate 1. (D) Larvae were trained with different concentrations of Rho_{extract} as a reward as shown on the right. The PIs of larvae trained with the Rho_{extract} significantly differed from the control, for which Rho_{extract} was omitted from the experiment (H -test, $P < 0.05$, $H = 21.6$, d.f. = 3, $N = 7, 9, 9, 9$; U -tests, $P < 0.05/3$ for all three Rho_{extract} concentrations tested versus control, 0.035 mg ml^{-1} : $U = 8.0$, 0.35 mg ml^{-1} : $U = 0$, 3.5 mg ml^{-1} : $U = 0$). 'b' indicates a significant difference from control ('a') in Bonferroni-corrected U -tests ($P < 0.05/3$) preceded by a Kruskal–Wallis test ($P < 0.05$). Other details as in Fig. 1. Data are documented in Table S3. Preference scores underlying the PIs are documented in Fig. S5.

Rhodiola* is rewarding to larval *Drosophila

Given the sensory attractiveness of *Rhodiola* to our experimental animals, we wondered whether it could also serve as a reward in a Pavlovian conditioning experiment. To test for such a rewarding effect, the odor AM was presented to separate groups of larvae, either paired or unpaired with *Rhodiola*. Then, the preference for the AM odor was measured, and the difference in preference between paired-trained and unpaired-trained groups of larvae was quantified through the associative PI. This revealed that *Rhodiola* had a rewarding effect at all three doses tested (Fig. 1C). Even the lowest dose used (0.1 mg ml^{-1}) was sufficient to establish memory that remained significant until 80 min after training (Fig. 1D). This rewarding effect and in particular the low dose at which it was observed were striking, because it was of about the same strength as fructose at a 2 mol l^{-1} concentration (360 mg ml^{-1}) (Fig. S1). Reducing the number of training trials from three to one confirmed the rewarding effect of *Rhodiola*, though as expected at lower levels and with less stable memory over time (Fig. 1E,F).

These strong rewarding effects of *Rhodiola* prompted us to venture into a bioassay-guided fractionation approach to identify the compounds that mediate this effect. Before doing so, however, we wanted to see whether an extract, i.e. soluble constituents of *Rhodiola*, might also be effective as a reward, and whether the neurogenetic 'fingerprint' of learning with such an extract corresponds to learning with more canonically used taste rewards.

Chemical properties and rewarding effect of the Rho_{extract}

From a 4 kg sample of *R. rosea* root material, an exhaustive extraction with 80% ethanol was performed. As shown by NMR, the resulting Rho_{extract} was dominated by sugars (Fig. 2A–C). Beside sucrose and glucose, a heptulose was also detected in MS measurements by ions at m/z 209 $[\text{M}-\text{H}]^-$, 245 $[\text{M}+\text{Cl}]^-$, 233 $[\text{M}+\text{Na}]^+$ and 249 $[\text{M}+\text{K}]^+$. The occurrence of sedoheptulose is a characteristic feature of Crassulaceae (Nordal, 1940). Given that the rewarding effect of *Rhodiola* was observed at doses much lower than those effective for sugars (Fig. 1; Schipanski et al., 2008; Rohwedder et al., 2012), it appeared very unlikely that these sugars mediate the rewarding effects of *Rhodiola*. We therefore performed a detailed MS analysis of the Rho_{extract} . This revealed the above-mentioned sugars and the occurrence of previously described characteristic, specialized metabolites such as phenylethanoid and phenylpropanoid glycosides like salidroside, rosavin and phenylethyl glycoside (Coors et al., 2019), monoterpene glycosides such as rosiridin, rhodiolside E and sacranoside A, cyanogenic glycosides such as lotaustralin, rhodiocyanosides A and B as well as gallic acid and derivatives (Fig. 2B,C and Table 3). The

glycosidic moieties of the observed monoglycosides (e.g. salidroside, ferulic acid glucoside) are most likely glucosides whereas diglycosides are suggested to contain 6- O - α -L-arabinopyranosyl- α -D-glucopyranoside, also found in the marker compound rosavin (Table 3). Interestingly, several of the major volatile compounds (phenylethanol, octanol, hexanol and myrtenol; Table 2) were also detected as their corresponding non-volatile glycosides. The broad band of background absorptions visible in the photodiode array (PDA) profile (Fig. 2B) is typical for *R. rosea* and might be due to epigallocatechin gallate oligomers (Panossian et al., 2010).

Behaviorally, presenting an odor together with Rho_{extract} revealed a strong and dose-dependent rewarding effect in larval *Drosophila* (Fig. 2D), indicating the extractability of rewarding compounds from *Rhodiola*. Therefore, subsequent analyses of this rewarding effect were performed with this Rho_{extract} .

Learning with Rho_{extract} does not require known dopaminergic reward neurons

Using the Rho_{extract} as the reward, we proceeded to investigate whether mushroom body function is required for Rho_{extract} learning (Fig. 3A). The mushroom bodies are situated at a side branch of the olfactory sensory-motor loop. They are largely dispensable for innate olfactory and gustatory behavior and feature a notably sparse multimodal representation of the sensory environment, including olfactory stimuli. Further, they receive intersecting input from distinct sets of modulatory neurons mediating punishment and reward information, respectively (Berck et al., 2016; Rohwedder et al., 2016; Eichler et al., 2017). A simplified working hypothesis of how odor–reward learning comes about is as follows. Upon odor-induced activation of the mushroom body neurons coincident with, for example, dopaminergic modulatory neurons mediating sugar reward information, an associative memory trace is formed. This takes place at the synapse from the odor-activated mushroom body neurons to their downstream partners, the mushroom body output neurons; signaling from these mushroom body output neurons eventually causes learned modulation of behavior (Pauls et al., 2010; Michels et al., 2011; Aso et al., 2014; Hige et al., 2015; Perisse et al., 2016; Rohwedder et al., 2016; Gerber and Aso, 2017; Saumweber et al., 2018). To see whether this working hypothesis is in principle also valid for odor– Rho_{extract} associative learning, the mushroom body neurons were silenced by transgenic expression of a hyperpolarizing GFP-tagged potassium channel ($MB^{OK107} > Kir^{GFP}$). This abolished odor– Rho_{extract} associative memory scores (Fig. 3B,C). In turn, silencing the mushroom body intrinsic GABAergic APL neurons, which arguably lifts inhibition of the mushroom body neurons and thus distorts the sparseness of the sensory representation, reduced memory scores by about a third (Fig. 3D,E). Whereas for silencing of the mushroom body neurons, impairment of innate odor preference might contribute to the reduced memory scores, this is not the case for silencing of the APL neurons (Fig. S2A,B). Of note is that the genetic controls did not show innate preference for the Rho_{extract} in the taste assay (Fig. S2C,D). On the one hand, this is unfortunate because it leaves tests of Rho_{extract} taste preference after silencing candidate neurons inconclusive. On the other hand, this lack of preference is informative. It suggests that the extraction protocol did not yield taste preference-promoting compounds (genetic controls in Fig. S2C,D), but did yield rewarding compounds (genetic controls in Fig. 3C,E,G,I), and thus suggests that different compounds mediate these two behavioral effects. We next sought to identify the rewarding compounds of the Rho_{extract} through bioassay-guided fractionation and AcorA (see above). This seemed particularly interesting because the silencing of those

Table 3. Ultra-high performance liquid chromatography (UHPLC)-HRESIMS characterization of *Rhodiola* crude extract (negative ionization)

Rt (min)	<i>m/z</i> , measured	Formula	Calculated	Annotation
0.27	209.0671 [M-H] [−]	C ₇ H ₁₃ O ₇	209.0667	Sedoheptulose
	245.0434 [M+Cl] [−]	C ₇ H ₁₄ O ₇ ³⁵ Cl		
0.27	341.1097 [M-H] [−]	C ₁₂ H ₂₁ O ₁₁	341.108	Sucrose
	377.0865 [M+Cl] [−]	C ₁₂ H ₂₂ O ₁₁ ³⁵ Cl	377.0856	
0.27	191.0196 [M-H] [−]	C ₆ H ₇ O ₇	191.0197	Citric acid
0.39	361.0785 [M-H] [−]	C ₁₄ H ₁₇ O ₁₁	361.0776	Galloyl sedoheptulose
0.41	331.0677 [M-H] [−]	C ₁₃ H ₁₅ O ₁₀	331.0660	Galloyl glucose
0.44	169.0147 [M-H] [−]	C ₇ H ₅ O ₅	169.0142	Gallic acid
0.73	329.0882 [M-H] [−]	C ₁₄ H ₁₇ O ₉	329.0878	Benzoic acid glucoside
0.85	304.1040 [M-H+HCOOH] [−]	C ₁₂ H ₁₈ NO ₈	304.1038	Rhodiocyanoside A
1.27	306.1195 [M-H+HCOOH] [−]	C ₁₂ H ₂₀ NO ₈	306.1195	Lotaustralin
1.42/1.60	299.1140 [M-H] [−]	C ₁₄ H ₁₉ O ₇	299.1136	Salidroside (tyrosol glucoside)
	345.1194 [M-H+HCOOH] [−]	C ₁₅ H ₂₁ O ₉	345.1191	
1.87	355.1035 [M-H] [−]	C ₁₆ H ₁₉ O ₉	355.1035	Ferulic acid glucoside
2.20	423.0935 [M-H] [−]	C ₁₉ H ₁₉ O ₁₁	423.0933	Hydroquinone galloyl glucoside
2.58	293.1247 [M-H+HCOOH] [−]	C ₁₂ H ₂₁ O ₈	293.1242	Isopentenyl glucoside
2.58	431.1565 [M-H] [−]	C ₁₉ H ₂₇ O ₁₁	431.1559	Tyrosol diglycoside*
3.04	426.1040 [M-H] [−]	C ₁₈ H ₂₀ NO ₁₁	426.1042	Rhodiocyanoside B
3.49	483.0779 [M-H] [−]	C ₂₀ H ₁₉ O ₁₄	483.0769	Digalloyl glucose
3.84/4.07	457.0777 [M-H] [−]	C ₂₂ H ₁₇ O ₁₁	457.0776	(epi)Gallocatechin gallates
4.22	401.1451 [M-H] [−]	C ₁₈ H ₂₅ O ₁₀	401.1442	Benzyl diglycoside*
	447.1506 [M-H+HCOOH] [−]	C ₁₉ H ₂₇ O ₁₂	447.1506	
4.48	197.0458 [M-H] [−]	C ₉ H ₉ O ₅	197.0455	Ethyl gallate
4.64	525.1981 [M-H] [−]	C ₂₅ H ₃₃ O ₁₂	525.1967	Neolignan glycoside
	571.2036 [M-H+HCOOH] [−]	C ₂₆ H ₃₅ O ₁₄	571.2036	
4.79	451.1254 [M-H] [−]	C ₂₁ H ₂₃ O ₁₁	451.1246	Galloyl salidroside
4.88	415.1614 [M-H] [−]	C ₁₉ H ₂₇ O ₁₀	415.1614	Phenylethyl diglycoside*
	461.1670 [M-H+HCOOH] [−]	C ₂₀ H ₂₉ O ₁₂	461.1670	
5.06	537.1981 [M-H+HCOOH] [−]	C ₂₆ H ₃₃ O ₁₂	537.1967	Lignan glycoside
5.17	331.1764 [M-H] [−]	C ₁₆ H ₂₇ O ₇	331.1762	Rosiridin
	377.1819 [M-H+HCOOH] [−]	C ₁₇ H ₂₉ O ₉	377.1817	
5.28	465.2341 [M-H] [−]	C ₂₁ H ₃₇ O ₁₁	465.2341	Rhodiolide E*
	511.2399 [M-H+HCOOH] [−]	C ₂₂ H ₃₉ O ₁₃	511.2396	
5.35	427.1616 [M-H] [−]	C ₂₀ H ₂₇ O ₁₀	427.1610	Rosavin*
	473.1670 [M-H+HCOOH] [−]	C ₂₁ H ₂₉ O ₁₂	473.1670	
5.38	449.2033 [M-H] [−]	C ₂₀ H ₃₃ O ₁₁		Octadienol diglucoside
	491.1927 [M-H] [−]	C ₂₅ H ₃₁ O ₁₀	491.1912	Lignan glycoside
	537.1982 [M-H+HCOOH] [−]	C ₂₆ H ₃₃ O ₁₂	537.1967	
5.47	395.1929 [M-H] [−]	C ₁₇ H ₃₁ O ₁₀	395.1923	Hexyl diglycoside*
	441.1984 [M-H+HCOOH] [−]	C ₁₈ H ₃₃ O ₁₂	441.1977	
5.56	261.1346 [M-H] [−]	C ₁₂ H ₂₁ O ₆	261.1333	Hexenyl glucoside
5.68	187.0978 [M-H] [−]	C ₉ H ₁₅ O ₄	187.0976	Fatty acid derivative
5.81	289.0721 [M-H] [−]	C ₁₅ H ₁₃ O ₆	289.0718	(epi)Catechin
6.12	421.2081 [M-H] [−]	C ₁₉ H ₃₃ O ₁₀	421.2070	Octenol diglycoside*
	467.2136 [M-H+HCOOH] [−]	C ₂₀ H ₃₅ O ₁₂	467.2134	
6.24	445.2084 [M-H] [−]	C ₂₁ H ₃₃ O ₁₀	445.2079	Myrtenol diglycoside* (sacranoside A)
	491.2141 [M-H+HCOOH] [−]	C ₂₂ H ₃₅ O ₁₂	491.2141	
6.36	447.2237 [M-H] [−]	C ₂₁ H ₃₅ O ₁₀	447.2236	Geraniol diglycoside*
	493.2292 [M-H+HCOOH] [−]	C ₂₂ H ₃₇ O ₁₂	493.2290	
6.59	423.2240 [M-H] [−]	C ₁₉ H ₃₅ O ₁₀	423.2236	Rhodiocyanoside*
	469.2295 [M-H+HCOOH] [−]	C ₂₀ H ₃₇ O ₁₂	469.2295	
7.03	273.0071 [M-H] [−]	C ₁₅ H ₁₃ O ₅	273.0768	Tetrahydroxyflavan
7.06	307.1191 [M-H] [−]	C ₁₆ H ₁₉ O ₆	307.1187	Feruloyloxy hexanoic acid
7.28	329.2333 [M-H] [−]	C ₁₈ H ₃₃ O ₅	329.2333	Lignan derivative
7.36	521.2753	C ₂₈ H ₄₁ O ₉	521.2745	
9.75	311.2229 [M-H] [−]	C ₁₈ H ₃₁ O ₄	311.2217	Dihydroxy octadecadienoic acid

*Diglycoside most likely corresponds to O-[α-L-arabinopyranosyl-(1→6)-β-D-glucopyranoside].

dopaminergic modulatory neurons that are required for sugar reward learning in the larva (Rohwedder et al., 2016; Saumweber et al., 2018) was without effect on memory through the *Rho*_{extract} reward (Fig. 3F–I). This suggests that the *Rho*_{extract} engages a ‘non-canonical’ reward pathway, potentially unrelated to sugar reward. If so, only the non-polar fractions of the *Rho*_{extract}, lacking most if not all sugars, should have a rewarding effect. The next experiment tested whether this was indeed the case.

Only the non-polar fractions of *Rho*_{extract} are rewarding

From the *Rho*_{extract} we performed successive liquid–liquid partitioning with solvents of different polarity. This resulted in four fractions (*Rho*_{water}, *Rho*_{butanol}, *Rho*_{ethyl acetate}, *Rho*_{heptane}) comprising substances from the *Rho*_{extract} separated by polarity (Fig. 4A,B) and partially overlapping with ‘neighboring’ fractions. The observed ¹H NMR spectra (Fig. 4B) confirm the predominant occurrence of free sugars in the most polar water fraction (*Rho*_{water}).

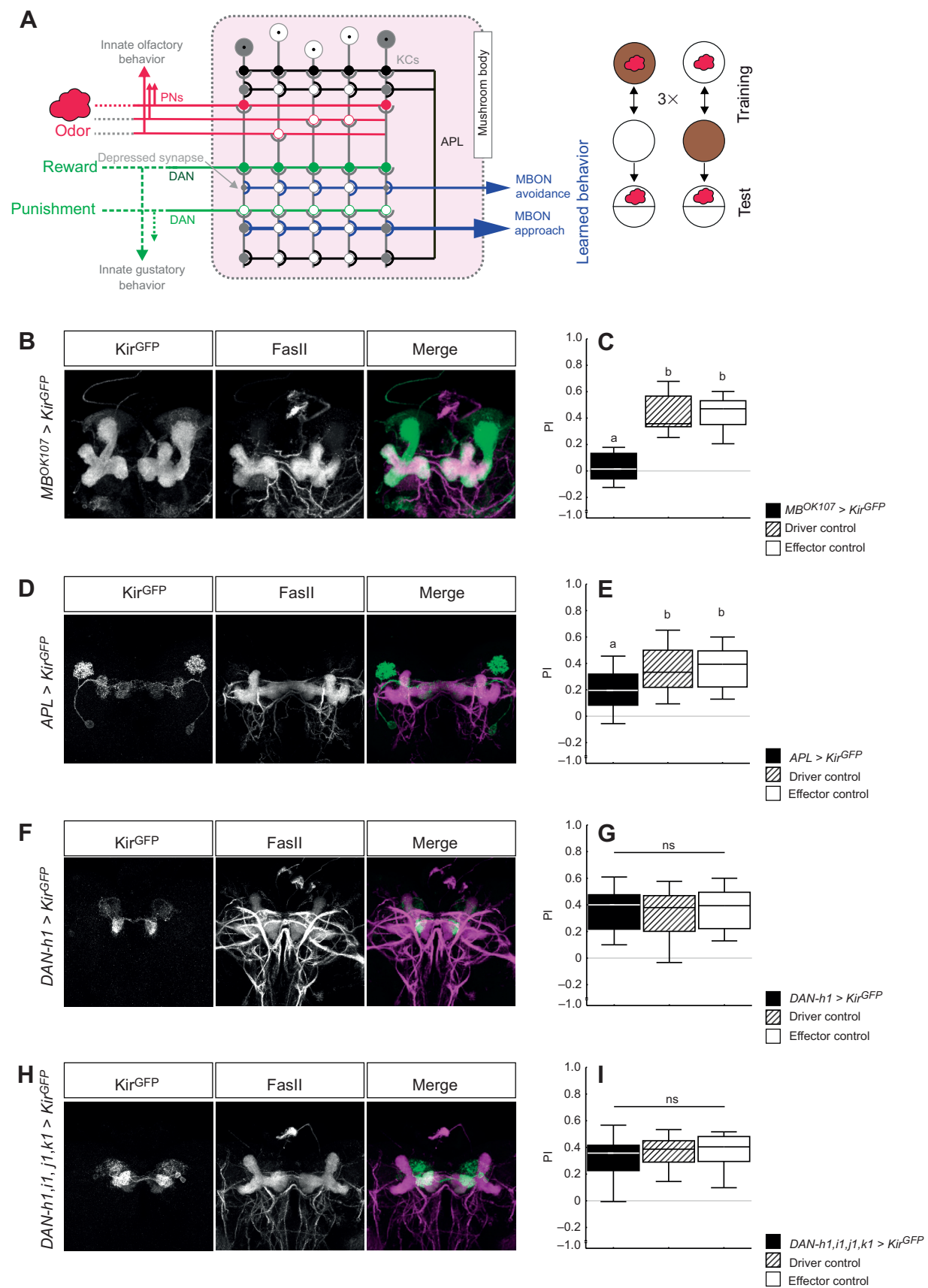


Fig. 3. See next page for legend.

Fig. 3. Learning with *Rho*_{extract} does not require known dopaminergic reward neurons. (A) Schematic circuits for appetitive olfactory learning. APL, GABAergic anterior paired lateral neuron; DAN, dopaminergic mushroom body input neuron; KCs, Kenyon cells; MBON, mushroom body output neurons; PNs, olfactory projection neurons. The small circles indicate KC-MBON synapses that are depressed as a result of the simultaneous presentation of odor and reward. For more details, please refer to the Results. The sketch on the right shows the behavioral paradigm used in C, E, G and I with 0.27 mg ml⁻¹ *Rho*_{extract} (brown) as the reward. (B) Brain of a *MB^{OK107}>Kir^{GFP}* larva stained with anti-GFP (left) and anti-FasII (middle) as counterstain, and the merge (right). (C) Memory scores of *MB^{OK107}>Kir^{GFP}* larvae were abolished and lower than in driver control and effector control larvae (*H*-test, $P<0.05$, $H=23.6$, d.f.=2, $N=13$, 13, 13; *U*-tests, *MB^{OK107}>Kir^{GFP}* versus driver control: $P<0.05/2$, $U=3.0$; *MB^{OK107}>Kir^{GFP}* versus effector control: $P<0.05/2$, $U=3.0$). (D) As in B, for *APL>Kir^{GFP}* larvae. (E) In *APL>Kir^{GFP}* larvae, memory scores were reduced (*H*-test, $P<0.05$, $H=15.0$, d.f.=2, $N=41$, 43, 36; *U*-tests, *APL>Kir^{GFP}* versus driver control: $P<0.05/2$, $U=514.5$; *APL>Kir^{GFP}* versus effector control: $P<0.05/2$, $U=407.0$). (F) As in B, for *DAN-h1>Kir^{GFP}* larvae. (G) When *DAN-h1* was silenced, memory scores remained intact (*DAN-h1>Kir^{GFP}*; *H*-test, $P>0.05$, $H=0.3$, d.f.=2, $N=15$, 16, 36). (H) As in B, for *DAN-h1*, *DAN-i1*, *DAN-j1*, *DAN-k1>Kir^{GFP}* (*DAN-j1* expression is stochastic across animals). (I) Silencing all four dopaminergic mushroom body input neurons innervating the medial lobe does not reduce memory scores (*H*-test, $P>0.05$, $H=2.3$, d.f.=2, $N=44$, 44, 44). ns: $P>0.05$ in Kruskal–Wallis tests. 'b' indicates a significant difference from the experimental group ('a') in Bonferroni-corrected *U*-tests ($P<0.05/2$) preceded by a Kruskal–Wallis test ($P<0.05$). Other details as in Fig. 1. Data are documented in Table S3. Preference scores underlying the PIs are documented in Fig. S6.

The neighboring *Rho*_{butanol} fraction contains in addition glycosidic compounds, gallic acid and galloyl derivatives, whereas the non-polar *Rho*_{ethyl acetate} and *Rho*_{heptane} fractions comprise aromatic compounds, phytosterols, fatty acids and fatty alcohols. Of these four fractions, only the *Rho*_{ethyl acetate} and the *Rho*_{heptane} fractions, i.e. the two non-polar ones, turned out to have a rewarding effect at low concentrations that exceeded the solvent control (Fig. 4C–F). The lack of a low-concentration rewarding effect in the *Rho*_{water} and *Rho*_{butanol} fractions specifically suggested that sugars, at the concentrations at which they are present in these fractions, are not sufficient as a reward. This is consistent with the previously reported dose–effect relationships for the rewarding effects of sugars (Schipanski et al., 2008; Rohwedder et al., 2012), and with the observation that silencing the dopamine neurons mediating sugar reward was without effect on the reward capacity of the *Rho*_{extract} (Fig. 3G,I).

Notably, only the most non-polar *Rho*_{heptane} fraction was effective as a reward at the lowest of the concentrations employed. This fraction does not contain any of the taste rewards known to be effective in *Drosophila* larvae (sugars, amino acids, sodium chloride) (Niewalda et al., 2008; Schipanski et al., 2008; Rohwedder et al., 2012; Schleyer et al., 2015). We were therefore curious whether further sub-fractionation of the two neighboring non-polar fractions would allow us to identify candidate substances hitherto not suspected of being rewarding.

Variance in the rewarding effect of sub-fractions allows candidate compounds to be identified

From the *Rho*_{ethyl acetate} and *Rho*_{heptane} fractions, another round of separation resulted in five and four sub-fractions (E1–E5 and H1–H4), respectively, which included partially overlapping sets of increasingly non-polar compounds (Fig. 4G). Using these nine sub-fractions at the same single concentration (3.35 µg ml⁻¹) in odor–reward associative learning experiments revealed that sub-fractions E5, H1 and H2 maintained a rewarding effect beyond solvent control levels. More importantly, these results yielded sufficient variance in memory scores between sub-fractions to relate them statistically to analytical data. To this end, we looked for correlations

of memory scores with the intensity of each analytical signal in all samples (AcorA). Specifically, the metabolite profiles of all fractions and sub-fractions were determined by direct-infusion ESI-FTICR-MS in positive ionization mode. Each analytical signal was characterized by a specific *m/z* value and intensity. After peak-picking and aligning these data, 936 different *m/z* features were detected across all samples (Table S2). To determine the correlation between memory scores and the mass signal intensities, the Spearman rank correlation coefficient was calculated, resulting in the identification of 51 positively correlating features (Table 1; Table S1). Based on these, the elemental composition of candidate compounds was calculated, which, through comparison with known natural products, allowed structure proposals for candidate compounds to be derived (Table 1; Table S1). Indeed, as the rewarding effects we had observed so far were not obviously getting successively weaker when *Rhodiola*, *Rho*_{extract}, the extract's non-polar fractions or the sub-fractions derived from these were used as the reward (Figs 1C, 2D and 4C–G), we felt encouraged to pick the most promising of these to see whether any of them might be rewarding in isolation, i.e. as a pure compound.

Identification of rewarding compounds

The correlating features from Table 1 and Table S1 suggest a high prevalence of mostly oxygenated fatty acid derivatives, sterol derivatives and terpenoids. In addition to the statistical correlation, we therefore compared the *Rho*_{extract} and all the above-mentioned fractions by TLC, HPLC, low- and high-resolution MS, and NMR (Fig. 4B). This indicated that all the active samples did indeed contain fatty acid, fatty alcohol or phytosterol derivatives. These compound classes were therefore considered to be particularly promising candidates for exerting a rewarding effect. We should note that the *Rhodiola* volatiles detected by GCMS (Table 2), and in particular phenylethanol as a major component, do not ionize under ESI conditions and could therefore not be included in the above ESI-MS analyses. NMR experiments, however, suggested the occurrence of phenylethanol and its derivatives in the non-polar fractions.

To determine the actual structure and verify the biological activity of the members of the candidate compound classes that correspond to the correlating structure proposals, isolation of the top candidates was attempted (Table 1; Table S1). Candidate 1 (*m/z* 485.36057; C₂₉H₅₀O₄Na⁺) and candidate 2 (*m/z* 365.26635; C₂₀H₃₈O₄Na⁺), which yielded the highest correlation coefficients, could not be obtained as pure compounds or enriched fractions. In contrast, it was possible to isolate candidate 3 (497.36086; C₃₀H₅₀O₄Na⁺) from the *Rho*_{ethyl acetate} fraction, and the structure was determined as ferulic acid eicosyl ester (FAE-20) (Michels et al., 2018). The isolated sample contained FAE-20 as a natural mixture of *trans* and *cis* isomers (3:1), accompanied by homologs bearing a shorter (C₁₈) or longer (C₂₂) even-numbered carbon alcohol chain.

The molecular formula of candidate 1 (C₂₉H₅₀O₄) differs from that of candidate 3 (C₃₀H₅₀O₄) by only one carbon, suggesting a structural similarity; however, in MS/MS experiments, the two compounds did not fragment in an analog manner. Whereas FAE-20 in the negative mode showed the predominant loss of a methyl moiety followed by loss of an extended series of neutral radicals differing by 14 u from the long alkyl chain (Schmidt et al., 2019), candidate 1 exhibited the loss of an acetyl function. The fragmentation in the positive mode was dominated by the loss of water (MS2), followed by the elimination of a C₁₈ alkyl chain (MS3) and an acetyl moiety (MS4). This fragmentation did not allow an unambiguous structure proposal for candidate 1, but excluded ferulic

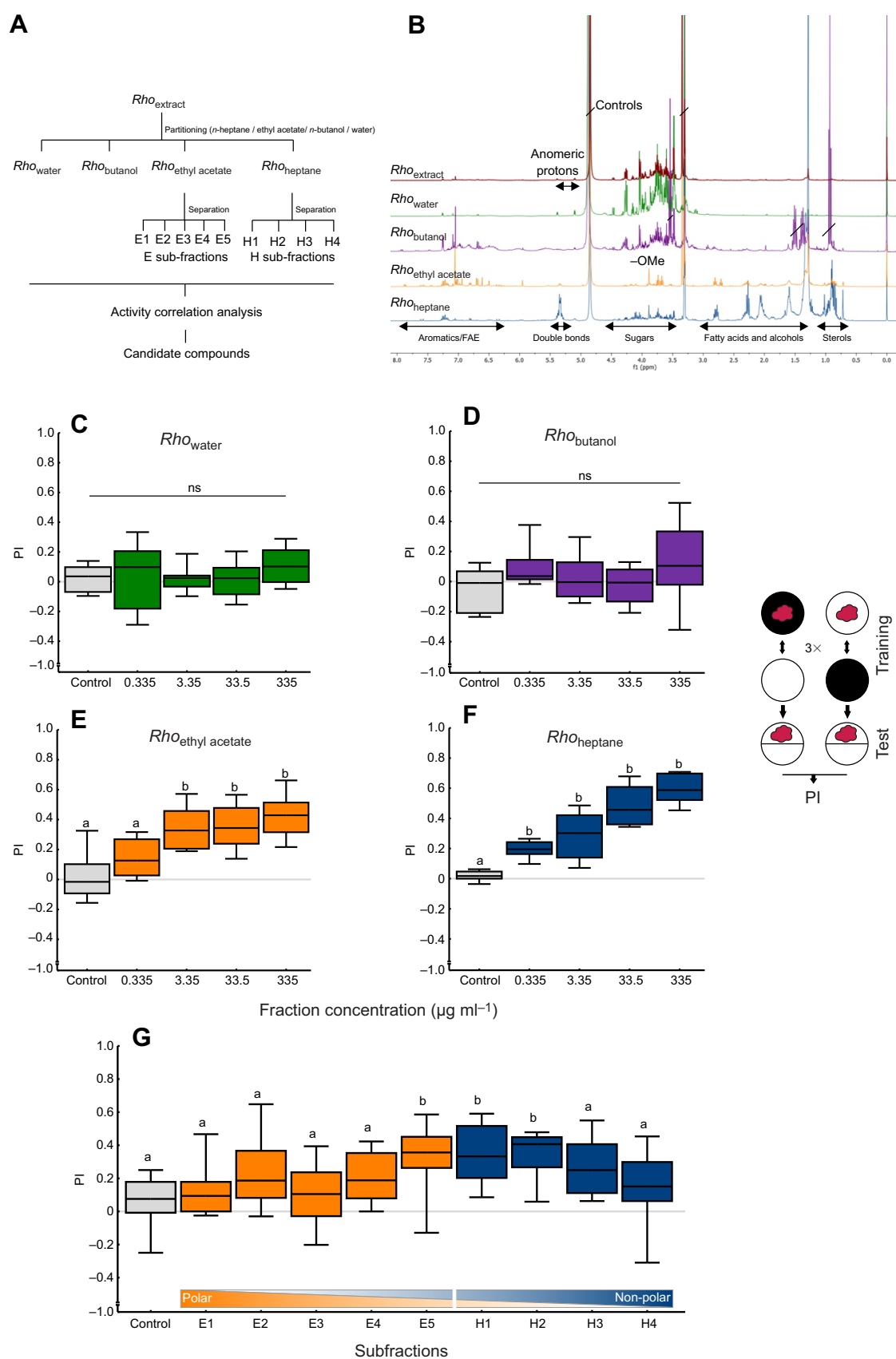


Fig. 4. See next page for legend.

Fig. 4. Bioassay-guided fractionation to identify candidate rewarding compounds in *Rhodiola* root. (A) Sketch of bioassay-guided fractionation. (B) ^1H NMR spectra of Rho_{extract} and partitioned fractions (measured in deuterated methanol, 400 MHz). The NMR spectra show the enrichment of sugars and glycosides in the polar fractions (Rho_{water} and Rho_{butanol}), and of sterols, fatty acids and fatty alcohols in the non-polar fractions ($Rho_{\text{ethyl acetate}}$ and Rho_{heptane}). The methoxyl group (–OMe) can be assigned to ferulic acid and derivatives (including FAE-20). (C–F) Larvae were trained with polarity-based fractions of the Rho_{extract} at the indicated concentrations, as the reward. The learning paradigm is sketched on the right. The two non-polar fractions, $Rho_{\text{ethyl acetate}}$ (E) and Rho_{heptane} (F), showed a rewarding effect ($Rho_{\text{ethyl acetate}}$: H -test, $P < 0.05$, $H = 28.8$, d.f. = 4, $N = 13$, 16, 13, 12, 12; U -test, $0.335 \mu\text{g ml}^{-1}$ versus control: $P > 0.05/4$, $U = 64.0$, $3.35 \mu\text{g ml}^{-1}$ versus control: $P < 0.05/4$, $U = 19.0$, $33.5 \mu\text{g ml}^{-1}$ versus control: $P < 0.05/4$, $U = 15.0$, $335 \mu\text{g ml}^{-1}$ versus control: $P < 0.05/4$, $U = 11.5$; Rho_{heptane} : H -test, $P < 0.05$, $H = 40.2$, d.f. = 4, $N = 12$, 12, 12, 12, 12; U -test, $0.335 \mu\text{g ml}^{-1}$ versus control: $P < 0.05/4$, $U = 13.0$, $3.35 \mu\text{g ml}^{-1}$ versus control: $P < 0.05/4$, $U = 14.0$, $33.5 \mu\text{g ml}^{-1}$ versus control: $P < 0.05/4$, $U = 9.0$, $335 \mu\text{g ml}^{-1}$ versus control: $P < 0.05/4$, $U = 0$). In contrast, neither Rho_{water} (C) nor Rho_{butanol} (D) had a rewarding effect (Rho_{water} : H -test, $P > 0.05$, $H = 3.6$, d.f. = 4, $N = 12$, 15, 14, 13, 12; Rho_{butanol} : H -test, $P > 0.05$, $H = 6.0$, d.f. = 4, $N = 12$, 12, 12, 12, 12). (G) Larvae were trained with $3.35 \mu\text{g ml}^{-1}$ of the sub-fractions separated from the $Rho_{\text{ethyl acetate}}$ fraction (E1–E5) and the Rho_{heptane} fraction (H1–H4). E1–E5 and H1–H4 yielded PIs that were significantly different from one another (H -test: $P < 0.05$, $H = 33.2$, d.f. = 9, $N = 14$, 15, 16, 16, 15, 15, 22, 21, 15, 15), with E5, H1 and H2 significantly different from the control (U -tests, E5 versus control: $P < 0.05/9$, $U = 34.0$; H1 versus control: $P < 0.05/9$, $U = 51.5$; H2 versus control: $P < 0.05/9$, $U = 38.0$). These results, combined with the metabolite distribution across active fractions and sub-fractions, allowed activity correlation analyses (AcorA) to be performed in order to derive candidate compounds (Table 1; Table S1; see Results). ns: $P > 0.05$ in Kruskal–Wallis test. 'b' indicates a significant difference from control ('a') in Bonferroni-corrected U -tests (C–F: $P < 0.05/4$, G: $P < 0.05/9$) preceded by a Kruskal–Wallis test ($P < 0.05$). Other details as in Fig. 1. Data are documented in Table S3. Preference scores underlying the PIs are documented in Fig. S7.

acid as a compound moiety. We note that nevertheless candidate 1 might belong to the group of alkyl hydroxycinnamates.

Additionally, further separation of the most active E5 sub-fraction, using column chromatography, yielded BSSG as its major constituent. Its $[\text{M}-\text{H}_2\text{O}+\text{Na}]^+$ peak at m/z 581.4182 appeared as correlating signal 46 (Table S1). Furthermore, fatty acids, fatty alcohols including eicosanol as the major compound, and stigmast-4-en-3-one were obtained as constituents of active sub-fractions. Because BSSG and FAE-20 isolated from *Rhodiola* exhibited a rewarding effect in low micromolar or even nanomolar concentrations, these two compounds were synthesized from commercially available starting material (Michels et al., 2018) and retested for their rewarding effect, which was indeed confirmed for both BSSG and FAE-20 (Fig. 5A–D).

Under acidic conditions, which are likely to occur along the alimentary canal upon ingestion and possibly also in the rotting-fruit habitat of larval *Drosophila*, esters might partly hydrolyze into an acid and an alcohol. We therefore wondered whether ferulic acid and 1-eicosanol, the products of the hydrolysis of FAE-20, would be effective as rewards. 1-Eicosanol was also found to be present in the fatty alcohol fraction isolated from an active sub-fraction (see Materials and Methods). The highest tested concentration of ferulic acid ($7.06 \mu\text{mol l}^{-1}$) was revealed to be more rewarding than the solvent control (Fig. 5E), whereas 1-eicosanol was without any such effect (Fig. 5F).

Similarly, sterol glycosides might be hydrolyzed into the aglycon and the sugar moiety. As mentioned above, sterol derivatives were regarded as potentially effective compounds. As representative compounds of this kind, BSSG and stigmast-4-en-3-one were isolated. The rewarding potential of commercially available stigmasterol, representing a common plant sterol structurally

closely related to sitosterol and stigmast-4-en-3-one, was therefore also evaluated; however, this did not show a rewarding effect (Fig. 5G).

To ascertain whether fatty acids can be considered candidate compounds that contribute to the observed rewarding effect, an isolated fatty acid fraction was also tested (Fig. 5H). Despite apparent trends, this did not have a rewarding effect beyond that of the solvent control at any of the concentrations used. According to NMR measurements, this fraction contains a mixture of unsaturated fatty acids with linoleic acid as the main compound (correlating signal 38; Table S1). Linoleic acid had previously been described as a major fatty acid in *R. rosea* (Pooja et al., 2006). However, MS experiments on this isolated fraction showed additional signals referring instead to oxygenated fatty acids that were also determined as correlating features (Table 1; e.g. 7: m/z 319 $[\text{M}+\text{Na}]^+$, linoleic acid+1 oxygen; 8: m/z 335 $[\text{M}+\text{Na}]^+$, linoleic acid+2 oxygens) (Fig. S3). Some of these might be lipid oxidation products arising in traces during storage of extracts. Their MS/MS fragmentation behavior is in accordance with hydroxylated fatty acids (e.g. Fig. S3B). We were not able to determine conclusive amounts or concentrations of these hydroxylated fatty acids in any of the fractions or sub-fractions by NMR experiments, or to enrich them during isolation. Taken together, the most plausible explanation for these results is that, because of their excellent ionization behavior in the electrospray ionization mass-spectrometric measurements (such as MS and MS/MS), even trace amounts of these substances might lead to false positive correlation results. Thus, the compound causing correlating signal 2 (m/z 365.26635 $[\text{M}+\text{Na}]^+$ $\text{C}_{20}\text{H}_{38}\text{O}_4\text{Na}^+$), which is in accordance with an oxygenated fatty acid, is also unlikely to be a promising candidate compound.

In conclusion, there is no evidence that fatty alcohols or unsaturated fatty acids, or oxygenated derivatives therefrom, exert a measurable rewarding effect in larval *Drosophila*. Rather, FAE-20, and to a lesser extent BSSG and ferulic acid are, as single compounds, rewarding to larval *Drosophila*.

DISCUSSION

Analytical chemistry of *R. rosea* root material

The volatile and non-volatile compounds from *R. rosea* root material identified here are consistent with previous reports. Specifically, to detect the volatile compounds, we used headspace GCMS focusing on major peaks, yielding results in good agreement with those of Rohloff (2002), who used headspace or steam distillate analysis. We did not identify decanol, though, which with related aliphatic alcohols may be responsible for the rubber-like background scent of *R. rosea* root material, whereas the remaining volatile substances, including the previously unreported linaloyl oxide and eucalyptol, might underlie its floral flavor. The non-volatile compounds detected here include phenylethanoid and phenylpropanoid glycosides, monoterpene glycosides, cyanogenic glycosides, gallic acid derivatives, sugars, sterols and fatty acids as previously reported (Brown et al., 2002; Panossian et al., 2010; Lee et al., 2016; Marchev et al., 2017). Notable is the high sedoheptulose content, a sugar that in its free form is a storage compound in Crassulaceae (Hegnauer, 1964; Ceusters et al., 2013).

To the best of our knowledge, ferulic acid or its derivatives have not so far been isolated from *R. rosea* although other phenolic acids such as benzoic, cinnamic, coumaric or caffeic acid have been reported (Panossian et al., 2010). However, ferulic acid has been shown to occur in *Rhodiola heterodonta* (Krasnov et al., 1976), and an ester of ferulic acid and hexanoic acid has been obtained from

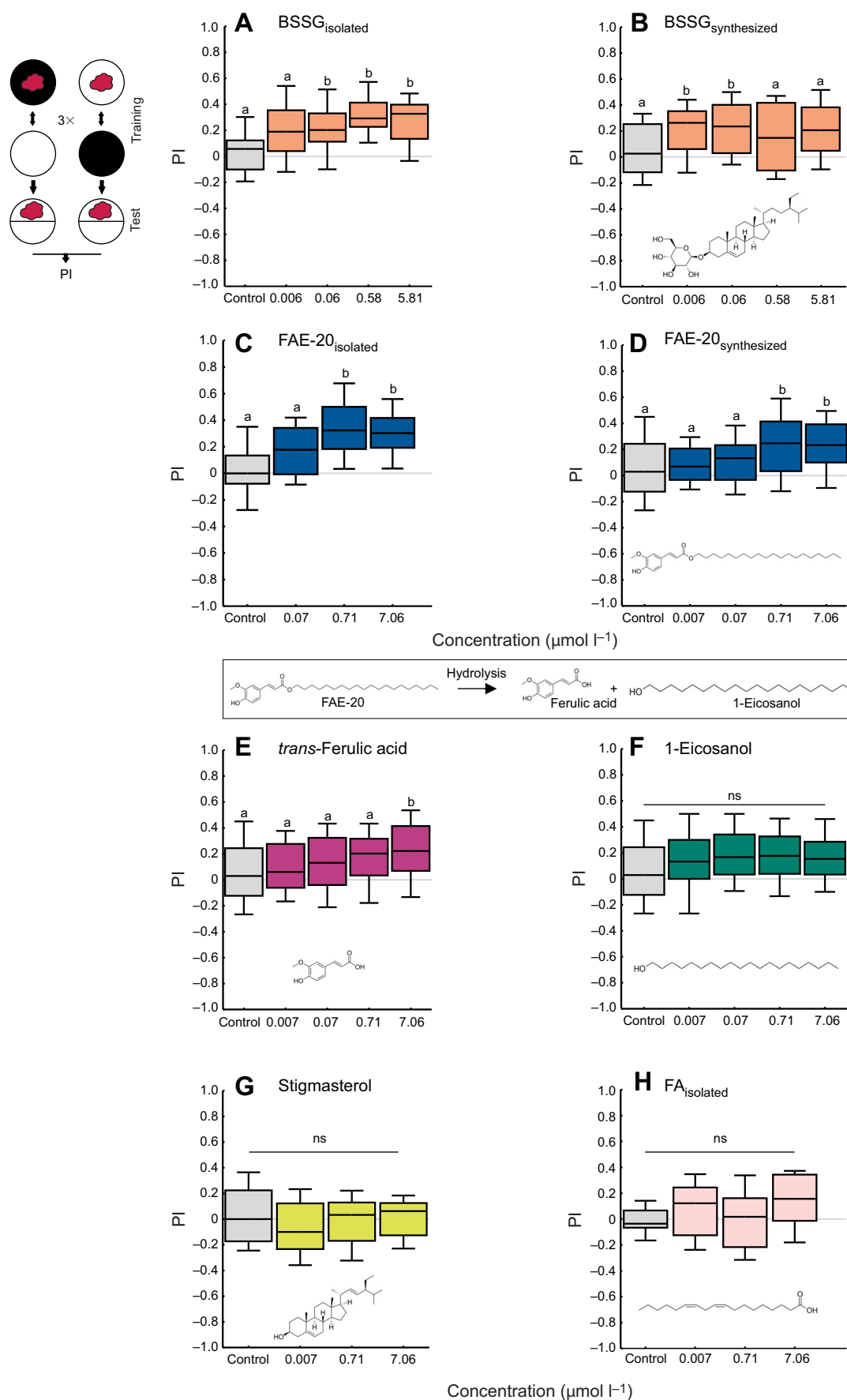


Fig. 5. See next page for legend.

Fig. 5. Confirming a rewarding effect of ferulic acid eicosyl ester (FAE-20), β -sitosterol- β -D-glucoside (BSSG) and ferulic acid. The results from Fig. 4, combined with the analysis of the metabolite distribution across active fractions and sub-fractions, suggested a number of candidate rewarding compounds (Table 1; Table S1; see Results). The most promising of these were then tested in isolated and synthesized form for their rewarding effect (sketch on the left; red cloud: *n*-amyl acetate, black circle: Petri dish with agarose supplemented with the candidate compound, white circle: plain agarose Petri dish). (A) Larvae were trained with the indicated concentrations of isolated BSSG (BSSG_{isolated}). Pls significantly differed between the groups (*H*-test, $P < 0.05$, $H = 15.9$, d.f.=4, $N = 16, 24, 16, 16, 22$), establishing appetitive memory scores in a concentration-dependent manner (*U*-tests, $0.006 \mu\text{mol l}^{-1}$ versus control: $P > 0.05/4$, $U = 107.0$; $0.06 \mu\text{mol l}^{-1}$ versus control: $P < 0.05/4$, $U = 59.0$; $0.58 \mu\text{mol l}^{-1}$ versus control: $P < 0.05/4$, $U = 32.0$; $5.81 \mu\text{mol l}^{-1}$ versus control: $P < 0.05/4$, $U = 73.5$). (B) Synthesized BSSG (BSSG_{synthesized}) in low micromolar concentrations was also effective as a reward (*H*-test, $P < 0.05$, $H = 9.6$, d.f.=4, $N = 35, 30, 31, 31, 32$; *U*-tests, $0.006 \mu\text{mol l}^{-1}$ versus control: $P < 0.05/4$, $U = 331.0$; $0.06 \mu\text{mol l}^{-1}$ versus control: $P < 0.05/4$, $U = 330.5$; $0.58 \mu\text{mol l}^{-1}$ versus control: $P > 0.05/4$, $U = 428.0$; $5.81 \mu\text{mol l}^{-1}$ versus control: $P > 0.05/4$, $U = 383.0$). (C,D) Pls of larvae when isolated FAE-20 (FAE-20_{isolated}; C) or synthesized FAE-20 (FAE-20_{synthesized}; D) was used as a reward. Both FAE-20_{isolated} and FAE-20_{synthesized} were effective as a reward (FAE-20_{isolated}: *H*-test, $P < 0.05$, $H = 27.6$, d.f.=3, $N = 30, 24, 24, 25$; *U*-tests, $0.07 \mu\text{mol l}^{-1}$ versus control: $P > 0.05/3$, $U = 230.5$; $0.71 \mu\text{mol l}^{-1}$ versus control: $P < 0.05/3$, $U = 106.0$; $7.06 \mu\text{mol l}^{-1}$ versus control: $P < 0.05/3$, $U = 130.5$; FAE-20_{synthesized}: *H*-test, $P < 0.05$, $H = 19.2$, d.f.=4, $N = 69, 33, 44, 45, 45$; *U*-tests, $0.007 \mu\text{mol l}^{-1}$ versus control: $P > 0.05/4$, $U = 1060.5$; $0.07 \mu\text{mol l}^{-1}$ versus control: $P > 0.05/4$, $U = 1286.5$; $0.71 \mu\text{mol l}^{-1}$ versus control: $P < 0.05/4$, $U = 1035.0$; $7.06 \mu\text{mol l}^{-1}$ versus control: $P < 0.05/4$, $U = 993$). (E,F) *trans*-Ferulic acid (E) but not 1-eicosanol (F), both of which are products of FAE-20 hydrolysis, has a rewarding effect (*trans*-ferulic acid: *H*-test, $P < 0.05$, $H = 13.2$, d.f.=4, $N = 69, 30, 43, 42, 42$; *U*-tests, $0.007 \mu\text{mol l}^{-1}$ versus control: $P > 0.05/4$, $U = 901.0$; $0.07 \mu\text{mol l}^{-1}$ versus control: $P > 0.05/4$, $U = 1273.5$, $0.71 \mu\text{mol l}^{-1}$ versus control: $P > 0.05/4$, $U = 1081.0$, $7.06 \mu\text{mol l}^{-1}$ versus control: $P < 0.05/4$, $U = 935.5$; 1-eicosanol: *H*-test, $P > 0.05$, $H = 9.4$, d.f.=4, $N = 69, 27, 51, 42, 45$). (G,H) The candidate compound stigmasterol (a common plant sterol; G) and a fraction of the active *Rho*_{heptane} H3 sub-fraction consisting mainly of fatty acids (FA_{isolated}; H) have no rewarding effect (stigmasterol: *H*-test, $P > 0.05$, $H = 1.80$, d.f.=3, $N = 17, 17, 17, 17$; FA_{isolated}: *H*-test, $P > 0.05$, $H = 7.5$, d.f.=3, $N = 27, 25, 24, 22$). ns: $P > 0.05$ in Kruskal–Wallis tests. 'b' indicates a significant difference from control ('a') in Bonferroni-corrected *U*-tests ($P < 0.05/4$ in A, B, D, E and $P < 0.05/3$ in C) preceded by Kruskal–Wallis tests ($P < 0.05$). Other details as in Fig. 1. Data are documented in Table S3. Preference scores underlying the Pls are documented in Fig. S8.

Rhodiola wallichiana (Song et al., 2018). Importantly, we recently described FAE-20 (Michels et al., 2018) as a bioactive constituent of *R. rosea*. This compound has not been detected in Crassulaceae before but has been found in the rhizomes of *Zingiber ottensii* (Zingiberaceae) (Akiyama et al., 2006), in the stem bark of *Pavetta owariensis* (Rubiaceae) (Baldé et al., 1991) and in *Baccharis genistelloides* (Asteraceae) (Hennig et al., 2011). Related alkyl hydroxycinnamates, typically consisting of the phenylpropanoids coumaric, caffeic or ferulic acid esterified with fatty alcohols of different chain length, are often found in association with plant lipid barriers such as cuticles and periderm in plant bark and roots, suggesting an involvement in suberin formation (Domergue and Kosma, 2017). Therefore, their occurrence might be expected in other folk-medicine plant roots with similar effects, such as ginseng (*Panax ginseng*), taiga root (*Eleutherococcus senticosus*) or maca root (*Lepidium meyenii*).

Rewarding compounds identified from *R. rosea*

The current study ascertained rewarding effects exerted by FAE-20, BSSG and ferulic acid. This does not rule out the possibility that further compounds from the non-polar fractions or their mixtures might also have rewarding effects, in particular at higher concentrations.

Ferulic acid and related compounds constitute dietary polyphenolic antioxidants present in fruits that can counteract oxidative stress in wild *Drosophila* populations (Dweck et al., 2015). Flies and larvae are unable to smell ferulic acid directly, but are attracted to antioxidant-containing food by yeast-produced volatiles, including ethylphenols, particularly ferulic acid-derived 4-ethyl guaiacol. The yeast bouquet also contains phenylethyl alcohol found in the headspace of *R. rosea*, probably contributing to the attraction shown by the larvae in the *Rhodiola* odor preference test. Furthermore, the esterification of ferulic acid with eicosanol might increase the volatility of the compound, potentially influencing its attractiveness to *Drosophila*.

BSSG, the glucoside of the most prominent phytosterol sitosterol, is a common plant constituent (for *R. rosea*: Kurkin et al., 1985; Kurkin et al., 1991). Its rewarding effect in *Drosophila* is surprising as BSSG can be found in other plants that so far have not been flagged as particularly attractive or rewarding to fruit flies. In fact, BSSG is known as a bioavailability improver, so its effect might be indirect (Bin Sayeed et al., 2016). In humans, phytosterol consumption is associated with cholesterol-lowering effects (Brufau et al., 2008). Further, phytosterol glycosides structurally resemble corticosteroids involved in the protective inactivation of the stress system (Panossian and Wikman, 2010). Notably, the long-term uptake of high amounts of BSSG as found in cycad seeds (*Cycas micronesica*) has been reported to exert neurotoxic effects (Tabata et al., 2008).

Compared with the sugars known to be rewarding in larval *Drosophila*, BSSG, ferulic acid and FAE-20 are effective at remarkably low concentrations. Whereas all three identified substances act in the low or sub-micromolar range, the sugars sucrose and fructose show their rewarding potency only at low molar concentrations (0.02 and 0.2 mol l^{-1} , respectively) (Schipanski et al., 2008; Rohwedder et al., 2012). The sugars glucose, xylose, arabinose and maltodextrin are effective as a reward in the same molar range, with maltodextrin and arabinose being effective at a slightly higher concentration of 1 and 2 mol l^{-1} , respectively (Rohwedder et al., 2012).

For salt (NaCl), rewarding effects have been observed for the low molar range, whereas increasing salt concentration changes it to a punishing effect (Niewalda et al., 2008), consistent with our own cooking experiences.

Furthermore, most if not all amino acids can have a rewarding effect (Kudow et al., 2017), but only for aspartic acid is a dose-effect function available, indicating a rewarding effect in the millimolar range (Schleyer et al., 2015).

Thus, the effective rewarding concentrations of BSSG, ferulic acid and FAE-20 are notably lower than for all previously known taste rewards. These known taste rewards are all water soluble and would all be contained in the polar fractions of the *Rho*_{extract}. Moreover, they are all in themselves of value to the larvae for energy production (sugars), growth (amino acids) and homeostasis (salt). Neither the low effective dose nor the chemical structures of BSSG, ferulic acid and FAE-20 suggest any such direct biological value. Rather, their rewarding effect may come about pharmacologically, more akin to other secondary (specialized) plant metabolites such as nicotine, caffeine or cocaine. While the molecular targets of *Rhodiola*, BSSG, ferulic acid and FAE-20 remain unknown, we might expect membrane interactions in the case of BSSG and FAE-20. Both compounds show an amphiphilic structure consisting of a hydrophilic side (glucose moiety or ferulic acid, respectively) and a hydrophobic part (sterol skeleton or alkyl chain). Phytosterols and their glycosides are typical constituents of plant plasma membranes that regulate membrane fluidity and permeability (Brufau et al.,

2008; Ferrer et al., 2017). The sugar part is probably located in the plane of the polar head groups of the membrane whereas the sterol moiety is integrated into the hydrophobic core of the lipid bilayer (Ferrer et al., 2017).

Neuronal mechanisms of reinforcement through *Rhodiola*

Interestingly, the neuronal requirements for the rewarding effect of the *Rho*_{extract} only partially overlap with those for odor–sugar reward learning (Fig. 3A). In both cases, intact mushroom body Kenyon cells as well as a functional APL neuron are required (Michels et al., 2011; Saumweber et al., 2018; Thum and Gerber, 2018; Lyutova et al., 2019; Zhou et al., 2019) but different neurons are apparently required to carry reward information to the mushroom body Kenyon cells. That is, silencing one of the dopaminergic input neurons to the medial lobe of the mushroom body, namely DAN-h1, impairs odor–fructose associative memory scores (Saumweber et al., 2018), but leaves the rewarding effect of the *Rho*_{extract} intact (Fig. 3G). Indeed, the silencing of all medial lobe DANs was inconsequential when *Rho*_{extract} was used as the reward (Fig. 3I), whereas this abolishes odor–fructose as well as odor–arabinose and odor–sorbitol memory scores (Rohwedder et al., 2016). Thus, given the above results, and given that DANs outside the medial lobe are apparently involved in aversive rather than appetitive learning (Eschbach et al., 2020), the remaining candidates are octopaminergic/tyraminerbic mushroom body input neurons (see also Hammer, 1993; Schroll et al., 2006; Eichler et al., 2017; Saumweber et al., 2018) and mushroom body input neurons with as yet unknown transmitters (MBIN-b1 and -b2, MBIN-c1, MBIN-l1, MBIN-e2).

Implications of the rewarding effect of FAE-20

Food supplementation with *Rhodiola* or the *Rho*_{extract} has an enhancing effect on odor–sugar associative memory in larval and aged *Drosophila*, and in bees (Michels et al., 2018). Furthermore, one of the compounds identified as rewarding in the present study, FAE-20, also has such a memory-enhancing effect in larval and aged adult *Drosophila*, and in aged mice as well (Michels et al., 2018). Thus, on the one hand *Rhodiola*, the *Rho*_{extract} and FAE-20 have a memory-enhancing effect that in humans would be welcome in cases of impaired mnemonic function. On the other hand, the present study shows that in larval *Drosophila* at least, they also have a strong rewarding effect. Should this be the case in humans, too, derivatives of FAE-20 should be sought that maintain its memory-enhancing effect but are not rewarding and are thus less likely to induce habitual use or addiction. In the search for such derivatives, the genetic tractability of *Drosophila* may allow for an accelerated analysis of the differential mechanisms underlying memory enhancement and the rewarding effect of FAE-20.

Acknowledgements

We thank S. Lenuweit, M. Wurm, A. Sibinski, V. Menne and F. Gerstner for experimental help, T. Saumweber for discussions, R. D. V. Glasgow for language editing, B. Westermann and A. Schaks for their contribution to chemical syntheses, and J. Schmidt for MS experiments.

Competing interests

B.M., K.F., L.A.W. and B.G. filed a patent to the German Patent and Trade Mark Office covering the application of FAE-20 for improving learning and memory.

Author contributions

Conceptualization: B.M., B.G., L.A.W.; Methodology: K.F., H.S., B.G., L.A.W.; Formal analysis: B.M., K.F.; Investigation: B.M., K.F., A.W., H.S.; Resources: B.M., L.A.W.; Data curation: B.M., K.F., H.S., B.G., L.A.W.; Writing - original draft: B.M., K.F., A.W., H.S., B.G., L.A.W.; Writing - review & editing: B.M., K.F., B.G., L.A.W.; Visualization: B.M., K.F., A.W., B.G.; Supervision: B.G., L.A.W.; Project administration: B.G., L.A.W.; Funding acquisition: B.G., L.A.W.

Funding

Institutional support was provided by Leibniz Institute for Neurobiology, Leibniz Institute of Plant Biochemistry, Leibniz Association, Otto-von-Guericke-University Magdeburg, State of Saxony-Anhalt. Project support was from German-Israeli Foundation for Scientific Research and Development Young Scientists' program, Leibniz Research Alliance Bioactive Compounds and Biotechnology (to B.M.), European Regional Development Fund (ZS/2016/05/78617 to L.W.). Overheads were from Deutsche Forschungsgemeinschaft (CRC779, GE1091/4-1, FOR2795 to B.G.).

Supplementary information

Supplementary information available online at <https://jeb.biologists.org/lookup/doi/10.1242/jeb.223982.supplemental>

References

- Akiyama, K., Kikuzaki, H., Aoki, T., Okuda, A., Lajis, N. H. and Nakatani, N. (2006). Terpenoids and a diarylheptanoid from *Zingiber ottensii*. *J. Nat. Prod.* **69**, 1637–1640. doi:10.1021/np0603119
- Arabit, J. G. J., Elhaj, R., Schriener, S. E., Sevrioukov, E. A. and Jafari, M. (2018). *Rhodiola rosea* improves lifespan, locomotion, and neurodegeneration in a *Drosophila melanogaster* model of Huntington's disease. *Biomed Res. Int.* **2018**, 6726874. doi:10.1155/2018/6726874
- Aso, Y., Sitaraman, D., Ichinose, T., Kaun, K. R., Vogt, K., Belliart-Guerin, G., Placais, P. Y., Robie, A. A., Yamagata, N., Schnaitmann, C., et al. (2014). Mushroom body output neurons encode valence and guide memory-based action selection in *Drosophila*. *Elife* **3**, e04580. doi:10.7554/eLife.04580.039
- Baldé, A. M., Claeys, M., Pieters, L. A., Wray, V. and Vlietinck, A. J. (1991). Ferulic acid esters from stem bark of *Pavetta owariensis*. *Phytochemistry* **30**, 1024–1026. doi:10.1016/0031-9422(91)85302-G
- Berck, M. E., Khandelwal, A., Claus, L., Hernandez-Nunez, L., Si, G., Tabone, C. J., Li, F., Truman, J. W., Fetter, R. D., Louis, M., et al. (2016). The wiring diagram of a glomerular olfactory system. *Elife* **5**, e14859. doi:10.7554/eLife.14859.022
- Bin Sayeed, M. S., Karim, S. M. R., Sharmin, T. and Morshed, M. M. (2016). Critical analysis on characterization, systemic effect, and therapeutic potential of beta-sitosterol: a plant-derived orphan phytosterol. *Medicines (Basel)* **3**, 29. doi:10.3390/medicines3040029
- Brown, R. P., Gerbarg, P. L. and Ramazanov, Z. (2002). *Rhodiola rosea*. A phytochemical overview. *HerbalGram* **56**, 40–52.
- Brufau, G., Canela, M. A. and Refecas, M. (2008). Phytosterols: physiologic and metabolic aspects related to cholesterol-lowering properties. *Nutr. Res.* **28**, 217–225. doi:10.1016/j.nutres.2008.02.003
- Ceusters, J., Godts, C., Peshev, D., Vergauwen, R., Dyubankova, N., Lescrinier, E., De Proft, M. P. and Van den Ende, W. (2013). Sedoheptulose accumulation under CO₂ enrichment in leaves of *Kalanchoe pinnata*: a novel mechanism to enhance C and P homeostasis? *J. Exp. Bot.* **64**, 1497–1507. doi:10.1093/jxb/ert010
- Connolly, J. B., Roberts, I. J. H., Armstrong, J. D., Kaiser, K., Forte, M., Tully, T. and O'Kane, C. J. (1996). Associative learning disrupted by impaired Gs signaling in *Drosophila* mushroom bodies. *Science* **274**, 2104–2107. doi:10.1126/science.274.5295.2104
- Coors, A., Brosch, M., Kahl, E., Khalil, R., Michels, B., Laub, A., Franke, K., Gerber, B. and Fendt, M. (2019). *Rhodiola rosea* root extract has antipsychotic-like effects in rodent models of sensorimotor gating. *J. Ethnopharmacol.* **235**, 320–328. doi:10.1016/j.jep.2019.02.031
- Degenhardt, A., Wittlake, R., Steilwind, S., Liebig, M., Runge, C., Hilmer, J. M., Krammer, G., Gohr, A., Wessjohann, L. A. (2014). Quantification of important flavour compounds in beef stocks and correlation to sensory results by 'Reverse Metabolomics'. In *Flavour Science* (ed. V. Ferreira), pp. 15–19. Amsterdam: Elsevier.
- Domergue, F. and Kosma, D. K. (2017). Occurrence and biosynthesis of alkyl hydroxycinnamates in plant lipid barriers. *Plants (Basel)* **6**, 25. doi:10.3390/plants6030025
- Dweck, H. K., Ebrahim, S. A., Farhan, A., Hansson, B. S. and Stensmyr, M. C. (2015). Olfactory proxy detection of dietary antioxidants in *Drosophila*. *Curr. Biol.* **25**, 455–466. doi:10.1016/j.cub.2014.11.062
- Eichler, K., Li, F., Litwin-Kumar, A., Park, Y., Andrade, I., Schneider-Mizell, C. M., Saumweber, T., Huser, A., Eschbach, C., Gerber, B., et al. (2017). The complete connectome of a learning and memory centre in an insect brain. *Nature* **548**, 175–182. doi:10.1038/nature23455
- Elameen, A., Dragland, S. and Klemesdal, S. S. (2010). Bioactive compounds produced by clones of *Rhodiola rosea* maintained in the Norwegian germplasm collection. *Pharmazie* **65**, 618–623.
- Eschbach, C., Fushiki, A., Winding, M., Schneider-Mizell, C. M., Shao, M., Arruda, R., Eichler, K., Valdes-Aleman, J., Ohyama, T., Thum, A. S., et al. (2020). Recurrent architecture for adaptive regulation of learning in the insect brain. *Nature Neurosci.* **24**, 544–555. doi:10.1038/s41593-020-0607-9

- European Medicines Agency (2012). Assessment report on *Rhodiola rosea* L., rhizoma et radix. http://www.ema.europa.eu/docs/en_GB/document_library/Herbal/_HMPC_assessment_report/2012/05/WC500127861.pdf.
- Faizi, S., Ali, M., Saleem, R., Irfanullah, R. and Bibi, S. (2001). Complete ¹H and ¹³C NMR assignments of stigma-5-en-3-O- β -glucoside and its acetyl derivatives. *Magn. Reson. Chem.* **39**, 399–405. doi:10.1002/mrc.855
- Ferrer, A., Altabella, T., Arro, M. and Boronat, A. (2017). Emerging roles for conjugated sterols in plants. *Prog. Lipid Res.* **67**, 27–37. doi:10.1016/j.plipres.2017.06.002
- Gerber, B. and Aso, Y. (2017). Localization, diversity and behavioral expression of associative engrams in *Drosophila*. *Learning Theory and Behavior* (ed. R. Menzel). In *Learning and Memory: A Comprehensive Reference*, Vol. 1, 2nd edn (ed. J. H. Byrne), pp. 463–473. Oxford: Elsevier.
- Gospodaryov, D. V., Yurkevych, I. S., Lushchak, O. V. and Lushchak, V. I. (2013). Lifespan extension and delay of age-related functional decline caused by *Rhodiola rosea* depends on dietary macronutrient balance. *Longev. Healthspan* **2**, 12. doi:10.1186/2046-2395-2-12
- Hammer, M. (1993). An identified neuron mediates the unconditioned stimulus in associative olfactory learning in honeybees. *Nature* **366**, 59–63. doi:10.1038/366059a0
- Hegnauer, R. (1964). *Chemotaxonomie der Pflanzen*, Vol. 3. Basel: Birkhäuser.
- Hennig, L., Garcia, G. M., Giannis, A. and Bussmann, R. W. (2011). New constituents of *Baccharis genistelloides* (Lam.) Pers. *Arkivoc* **2011**, 74–81. doi:10.3998/ark.5550190.0012.607
- Hielscher-Michael, S., Griehl, C., Buchholz, M., Demuth, H. U., Arnold, N. and Wessjohann, L. A. (2016). Natural products from microalgae with potential against Alzheimer's disease: sulfolipids are potent glutamyl cyclase inhibitors. *Mar. Drugs* **14**, 203–219. doi:10.3390/md14110203
- Hige, T., Aso, Y., Modi, M. N., Rubin, G. M. and Turner, G. C. (2015). Heterosynaptic plasticity underlies aversive olfactory learning in *Drosophila*. *Neuron* **88**, 985–998. doi:10.1016/j.neuron.2015.11.003
- Ishaque, S., Shamseer, L., Bukutu, C. and Vohra, S. (2012). *Rhodiola rosea* for physical and mental fatigue: a systematic review. *BMC Complement. Altern. Med.* **12**, 70. doi:10.1186/1472-6882-12-70
- Jafari, M., Felgner, J. S., Bussel, I. I., Hutchili, T., Khodayari, B., Rose, M. R., Vince-Cruz, C. and Mueller, L. D. (2007). *Rhodiola*: a promising anti-aging Chinese herb. *Rejuvenation Res.* **10**, 587–602. doi:10.1089/rej.2007.0560
- Krasnov, E. A., Bokova, V. S. and Pimenov, M. G. (1976). Phenolic compounds of *Rhodiola viridula* and *Rh. heterodonta*. *Chem. Nat. Compd.* **12**, 480–481. doi:10.1007/BF00564822
- Kudow, N., Miura, D., Schleyer, M., Toshima, N., Gerber, B. and Tanimura, T. (2017). Preference for and learning of amino acids in larval *Drosophila*. *Biol. Open* **6**, 365–369. doi:10.1242/bio.020412
- Kurkin, V. A., Zapesochay, G. G. and Shchavinskii, A. N. (1985). Terpenoids of the rhizomes of *Rhodiola rosea*. *Chem. Nat. Compd.* **21**, 593–597. doi:10.1007/BF00579060
- Kurkin, V. A., Zapesochay, G. G., Dubichev, A. G., Vorontsov, E. D., Aleksandrova, I. V. and Panova, R. V. (1991). Phenylpropanoids of a callus culture of *Rhodiola rosea*. *Chem. Nat. Compd.* **27**, 419–425. doi:10.1007/BF00636560
- Larsson, M. C., Domingos, A. I., Jones, W. D., Chiappe, M. E., Amrein, H. and Vossahl, L. B. (2004). Or83b encodes a broadly expressed odorant receptor essential for *Drosophila* olfaction. *Neuron* **43**, 703–714. doi:10.1016/j.neuron.2004.08.019
- Lee, T.-H., Hsu, C.-C., Hsiao, G., Fang, J.-Y., Liu, W.-M. and Lee, C.-K. (2016). Anti-MMP-2 activity and skin-penetrating capability of the chemical constituents from *Rhodiola rosea*. *Planta Med.* **82**, 698–704. doi:10.1055/s-0042-101033
- Linnaeus, C. (1749). *Materia medica*, Volume 1, *De plantis*, 168.
- Lytova, R., Selcho, M., Pfeuffer, M., Segebarth, D., Habenstein, J., Rohwedder, A., Frantzmam, F., Wegener, C., Thum, A. S. and Pauls, D. (2019). Reward signaling in a recurrent circuit of dopaminergic neurons and peptidergic Kenyon cells. *Nat. Commun.* **10**, 3097. doi:10.1038/s41467-019-11092-1
- Marchev, A. S., Aneva, I. Y., Koycheva, I. K. and Georgiev, M. I. (2017). Phytochemical variations of *Rhodiola rosea* L. wild-grown in Bulgaria. *Phytochem. Lett.* **20**, 386–390. doi:10.1016/j.phytol.2016.12.030
- Michels, B., Chen, Y.-C., Saumweber, T., Mishra, D., Tanimoto, H., Schmid, B., Engmann, O. and Gerber, B. (2011). Cellular site and molecular mode of synapsin action in associative learning. *Learn. Mem.* **18**, 332–344. doi:10.1101/lm.210141
- Michels, B., Saumweber, T., Biernacki, R., Thum, J., Glasgow, R. D. V., Schleyer, M., Chen, Y.-C., Eschbach, C., Stocker, R. F., Toshima, N., et al. (2017). Pavlovian conditioning of larval *Drosophila*: an illustrated, multilingual, hands-on manual for odor-taste associative learning in maggots. *Front. Behav. Neurosci.* **11**, 45. doi:10.3389/fnbeh.2017.00045
- Michels, B., Zwaka, H., Bartels, R., Lushchak, O., Franke, K., Endres, T., Fendt, M., Song, I., Bakr, M., Budragchaa, T., et al. (2018). Memory enhancement by ferulic acid ester across species. *Sci. Adv.* **4**, eaat6994. doi:10.1126/sciadv.aat6994
- Neuser, K., Husse, J., Stock, P. and Gerber, B. (2005). Appetitive olfactory learning in *Drosophila* larvae: effects of repetition, reward strength, age, gender, assay type and memory span. *Anim. Behav.* **69**, 891–898. doi:10.1016/j.anbehav.2004.06.013
- Niewald, T., Singhal, N., Fiala, A., Saumweber, T., Wegener, S. and Gerber, B. (2008). Salt processing in larval *Drosophila*: choice, feeding, and learning shift from appetitive to aversive in a concentration-dependent way. *Chem. Senses* **33**, 685–692. doi:10.1093/chemse/bjn037
- Nordal, A. (1940). Sedoheptose in Norwegian Crassulaceae. *Arch. Pharm.* **278**, 289–298.
- Panossian, A. and Wikman, G. (2010). Effects of adaptogens on the central nervous system and the molecular mechanisms associated with their stress-protective activity. *Pharmaceuticals (Basel)* **3**, 188–224. doi:10.3390/ph3010188
- Panossian, A., Wikman, G. and Sarris, J. (2010). *Rosenroot (Rhodiola rosea): traditional use, chemical composition, pharmacology and clinical efficacy. Phytomedicine* **17**, 481–493. doi:10.1016/j.phymed.2010.02.002
- Pauls, D., Selcho, M., Gendre, N., Stocker, R. F. and Thum, A. S. (2010). *Drosophila* larvae establish appetitive olfactory memories via mushroom body neurons of embryonic origin. *J. Neurosci.* **30**, 10655–10666. doi:10.1523/JNEUROSCI.1281-10.2010
- Perisse, E., Oswald, D., Barnstedt, O., Talbot, C. B., Huetteroth, W. and Waddell, S. (2016). Aversive learning and appetitive motivation toggle feed-forward inhibition in the *Drosophila* mushroom body. *Neuron* **90**, 1086–1099. doi:10.1016/j.neuron.2016.04.034
- Petkov, V. D., Yonkov, D., Mosharoff, A., Kambourova, T., Alova, L., Petkov, V. V. and Todorov, I. (1986). Effects of alcohol aqueous extract from *Rhodiola rosea* L. roots on learning and memory. *Acta Physiol. Pharmacol. Bulg.* **12**, 3–16.
- Pfeiffer, B. D., Ngo, T.-T. B., Hibbard, K. L., Murphy, C., Jenett, A., Truman, J. W. and Rubin, G. M. (2010). Refinement of tools for targeted gene expression in *Drosophila*. *Genetics* **186**, 735–755. doi:10.1534/genetics.110.119917
- Pooja, A. K. R., Khanum, F. and Bawa, A. S. (2006). Phytoconstituents and antioxidant potency of *Rhodiola rosea* – a versatile adaptogen. *J. Food Biochem.* **30**, 203–214. doi:10.1111/j.1745-4514.2006.00055.x
- Rohloff, J. (2002). Volatiles from rhizomes of *Rhodiola rosea* L. *Phytochemistry* **59**, 655–661. doi:10.1016/S0031-9422(02)00004-3
- Rohwedder, A., Pfizenmaier, J. E., Ramsperger, N., Apostolopoulou, A. A., Widmann, A. and Thum, A. S. (2012). Nutritional value-dependent and nutritional value-independent effects on *Drosophila melanogaster* larval behavior. *Chem. Senses* **37**, 711–721. doi:10.1093/chemse/bjs055
- Rohwedder, A., Wenz, N. L., Stehle, B., Huser, A., Yamagata, N., Zlatić, M., Truman, J. W., Tanimoto, H., Saumweber, T., Gerber, B., et al. (2016). Four individually identified paired dopamine neurons signal reward in larval *Drosophila*. *Curr. Biol.* **26**, 661–669. doi:10.1016/j.cub.2016.01.012
- Saumweber, T., Husse, J. and Gerber, B. (2011). Innate attractiveness and associative learnability of odors can be dissociated in larval *Drosophila*. *Chem. Senses* **36**, 223–235. doi:10.1093/chemse/bjq128
- Saumweber, T., Rohwedder, A., Schleyer, M., Eichler, K., Chen, Y.-C., Aso, Y., Cardona, A., Eschbach, C., Kobler, O., Voigt, A., et al. (2018). Functional architecture of reward learning in mushroom body extrinsic neurons of larval *Drosophila*. *Nat. Commun.* **9**, 1104. doi:10.1038/s41467-018-03130-1
- Scherer, S., Stocker, R. F. and Gerber, B. (2003). Olfactory learning in individually assayed *Drosophila* larvae. *Learn. Mem.* **10**, 217–225. doi:10.1101/lm.57903
- Schipanski, A., Yarali, A., Niewald, T. and Gerber, B. (2008). Behavioral analyses of sugar processing in choice, feeding, and learning in larval *Drosophila*. *Chem. Senses* **33**, 563–573. doi:10.1093/chemse/bjn024
- Schleyer, M., Miura, D., Tanimura, T. and Gerber, B. (2015). Learning the specific quality of taste reinforcement in larval *Drosophila*. *Elife* **4**, e04711. doi:10.7554/elife.04711
- Schmidt, J., Kuck, D., Franke, K., Sultani, H., Laub, A. and Wessjohann, L. A. (2019). The unusual fragmentation of long-chain feruloyl esters under negative ion electrospray conditions. *J. Mass Spectrom.* **54**, 549–556. doi:10.1002/jms.4357
- Schroll, C., Riemensperger, T., Bucher, D., Ehmer, J., Voller, T., Erbguth, K., Gerber, B., Hendel, T., Nagel, G., Buchner, E., et al. (2006). Light-induced activation of distinct modulatory neurons triggers appetitive or aversive learning in *Drosophila* larvae. *Curr. Biol.* **16**, 1741–1747. doi:10.1016/j.cub.2006.07.023
- Smith, C. A., Want, E. J., O'Maille, G., Abagyan, R. and Siuzdak, G. (2006). XCMS: processing mass spectrometry data for metabolite profiling using nonlinear peak alignment, matching, and identification. *Anal. Chem.* **78**, 779–787. doi:10.1021/ac051437y
- Song, Y., Zhou, J., Wang, X., Xie, X., Zhao, Y., Ni, F., Huang, W., Wang, Z. and Xiao, W. (2018). A new ferulic acid ester from *Rhodiola wallichiana* var. *cholaensis* (Crassulaceae). *Nat. Prod. Res.* **32**, 77–84. doi:10.1080/14786419.2017.1335724
- Tabata, R. C., Wilson, J. M., Ly, P., Zwieggers, P., Kwok, D., Van Kampen, J. M., Cashman, N. and Shaw, C. A. (2008). Chronic exposure to dietary sterol glucosides is neurotoxic to motor neurons and induces an ALS-PDC phenotype. *Neuromolecular Med.* **10**, 24–39. doi:10.1007/s12017-007-8020-z
- Thum, A. S. and Gerber, B. (2018). Connectomics and function of a memory network: the mushroom body of larval *Drosophila*. *Curr. Opin. Neurobiol.* **54**, 146–154. doi:10.1016/j.conb.2018.10.007
- Vossahl, L. B. and Hansson, B. S. (2011). A unified nomenclature system for the insect olfactory coreceptor. *Chem. Senses* **36**, 497–498. doi:10.1093/chemse/bjr022

- Weiglein, A., Gerstner, F., Mancini, N., Schleyer, M. and Gerber, B. (2019). One-trial learning in larval *Drosophila*. *Learn. Mem.* **26**, 109–120. doi:10.1101/lm.049106.118
- Wiegant, F. A. C., Surinova, S., Ytsma, E., Langelaar-Makkinje, M., Wikman, G. and Post, J. A. (2009). Plant adaptogens increase lifespan and stress resistance in *C. elegans*. *Biogerontology* **10**, 27–42. doi:10.1007/s10522-008-9151-9
- Zhou, M., Chen, N., Tian, J., Zeng, J., Zhang, Y., Zhang, X., Guo, J., Sun, J., Li, Y., Guo, A., et al. (2019). Suppression of GABAergic neurons through D2-like receptor secures efficient conditioning in *Drosophila* aversive olfactory learning. *Proc. Natl. Acad. Sci. USA* **116**, 5118–5125. doi:10.1073/pnas.1812342116

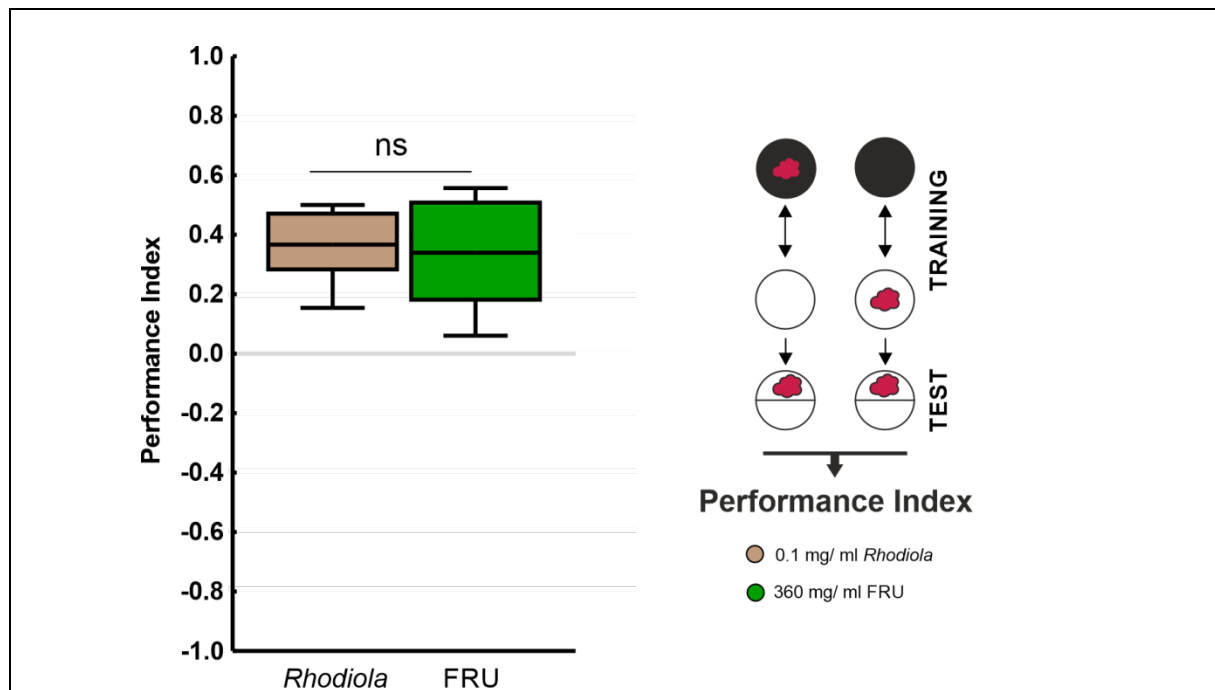


Fig. S1: Comparing reward strength of *Rhodiola* root and fructose

Shown are associative memory scores measured as the Performance Indices of larvae trained with either 0.1 mg/ml *Rhodiola* root or 2 mol/l fructose (= 360 mg/ml, FRU) as the reward (sketch to the right, red cloud: odor *n*-amyl acetate, black circles: Petri dishes filled with agarose supplemented with *Rhodiola* or FRU, white circles: plain agarose Petri dishes). The Performance Indices of larvae trained with 0.1 mg/ml *Rhodiola* or FRU did not significantly differ from each other (U-test, $P > 0.05$, $U = 191.5$, $N = 21, 20$). ns: $P > 0.05$ in a U-test. Other details as in Fig. 1. Data are documented in *Data file S2 Behavior data.xlsx*. Preference scores underlying the Performance Indices are documented in Fig. S9.

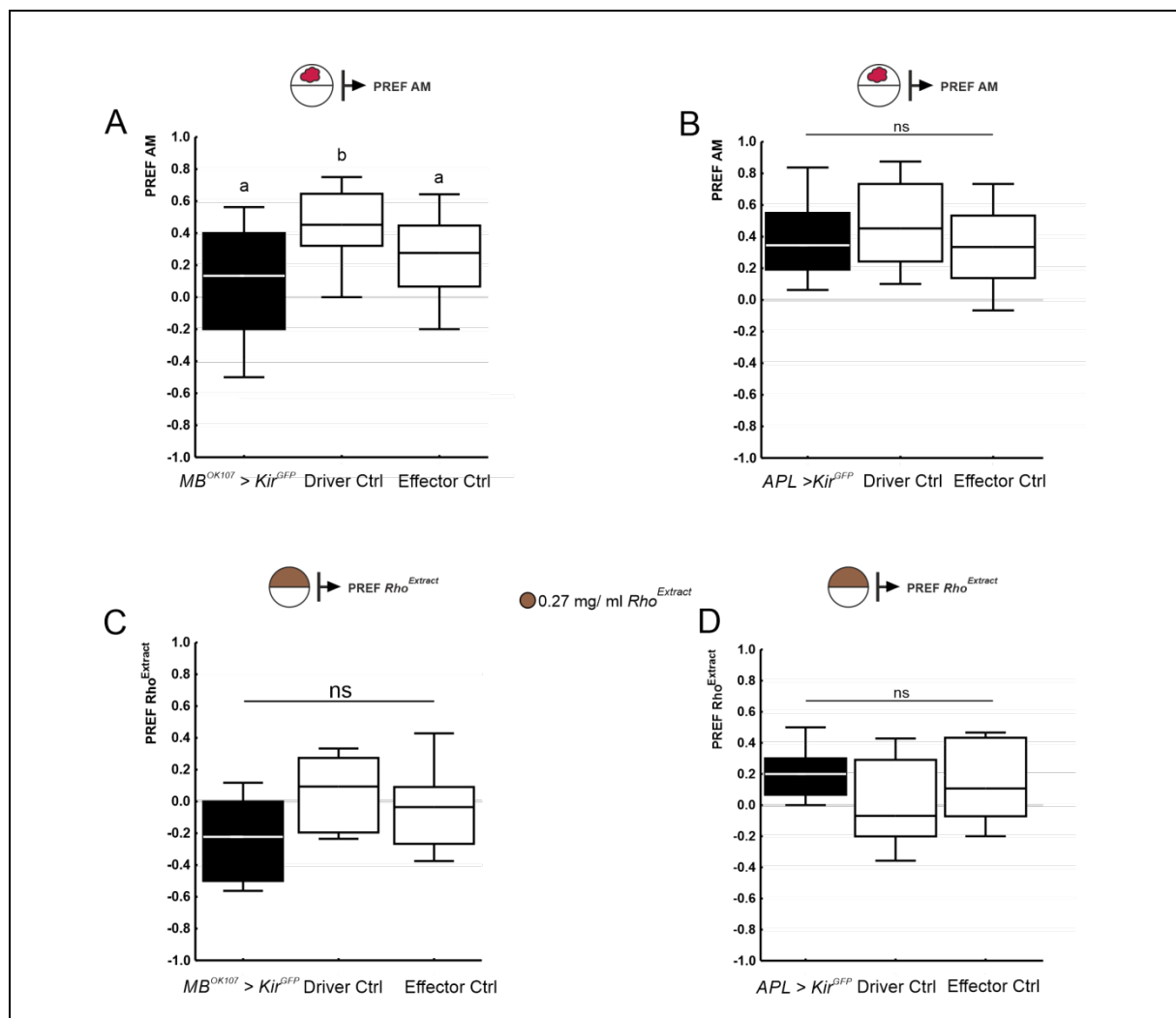


Fig. S2: Silencing of mushroom body neurons does not affect task-relevant sensory-motor faculties

Shown are the preference scores of experimentally naïve larvae in the sketched preference paradigms for the odor *n*-amyl acetate (AM; red cloud) (A, B), as well as for the $Rho^{Extract}$ (brown hemicircle: $Rho^{Extract}$ -supplemented agarose) (C, D), for the experimental groups $MB^{OK107} > Kir^{GFP}$ (A and C) and $APL > Kir^{GFP}$ (B and D) with their respective genetic controls. In neither case is the experimental group significantly different from both controls. *n*-amyl acetate: (A) H-test, $P < 0.05$, $H = 14.2$, $df = 2$, $N = 28, 28, 28$; U-tests, $MB^{OK107} > Kir^{GFP}$ vs. Driver Ctrl: $P < 0.05/2$, $U = 176.5$; $MB^{OK107} > Kir^{GFP}$ vs. Effector Ctrl: $P > 0.05/2$, $U = 300.5$; (B) H-test, $P > 0.05$, $H = 2.3$, $df = 2$, $N = 20, 20, 20$. *Rhodiola*: (C) H-test, $P > 0.05$, $H = 3.4$, $df = 2$, $N = 6, 12, 14$; (D) H-test, $P > 0.05$, $H = 2.3$, $df = 2$, $N = 12, 12, 12$). ns: $P > 0.05$ in a Kruskal-Wallis test. 'b' indicates a significant difference from the experimental group ('a') in Bonferroni-corrected U-tests ($P < 0.05/2$) preceded by a Kruskal-Wallis test ($P < 0.05$). Other details as in Fig. 1. Data are documented in *Data file S2 Behavior data.xlsx*.

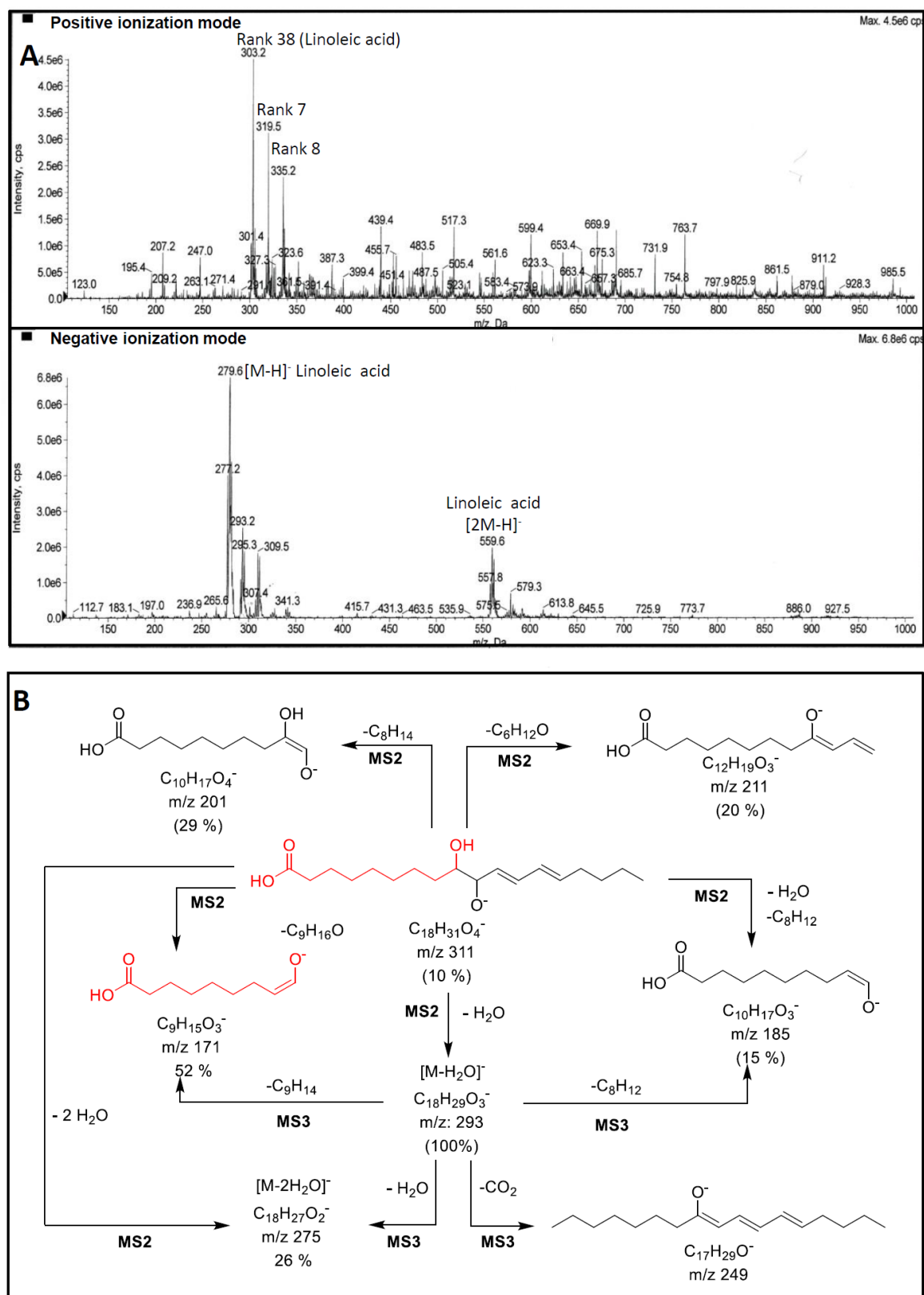


Fig. S3: ESI-MS data of *Rhodiola* fatty acids

A) ESI-MS spectrum of the fatty acid fraction isolated from *Rhodiola* documenting the occurrence of oxygenated derivatives. B) Negative MS/MS fragmentation pattern of the hydroxylated fatty acid derivative hit 8 is in accordance with the structure proposal 9,10-dihydroxy-11,13-octadecadienic acid.

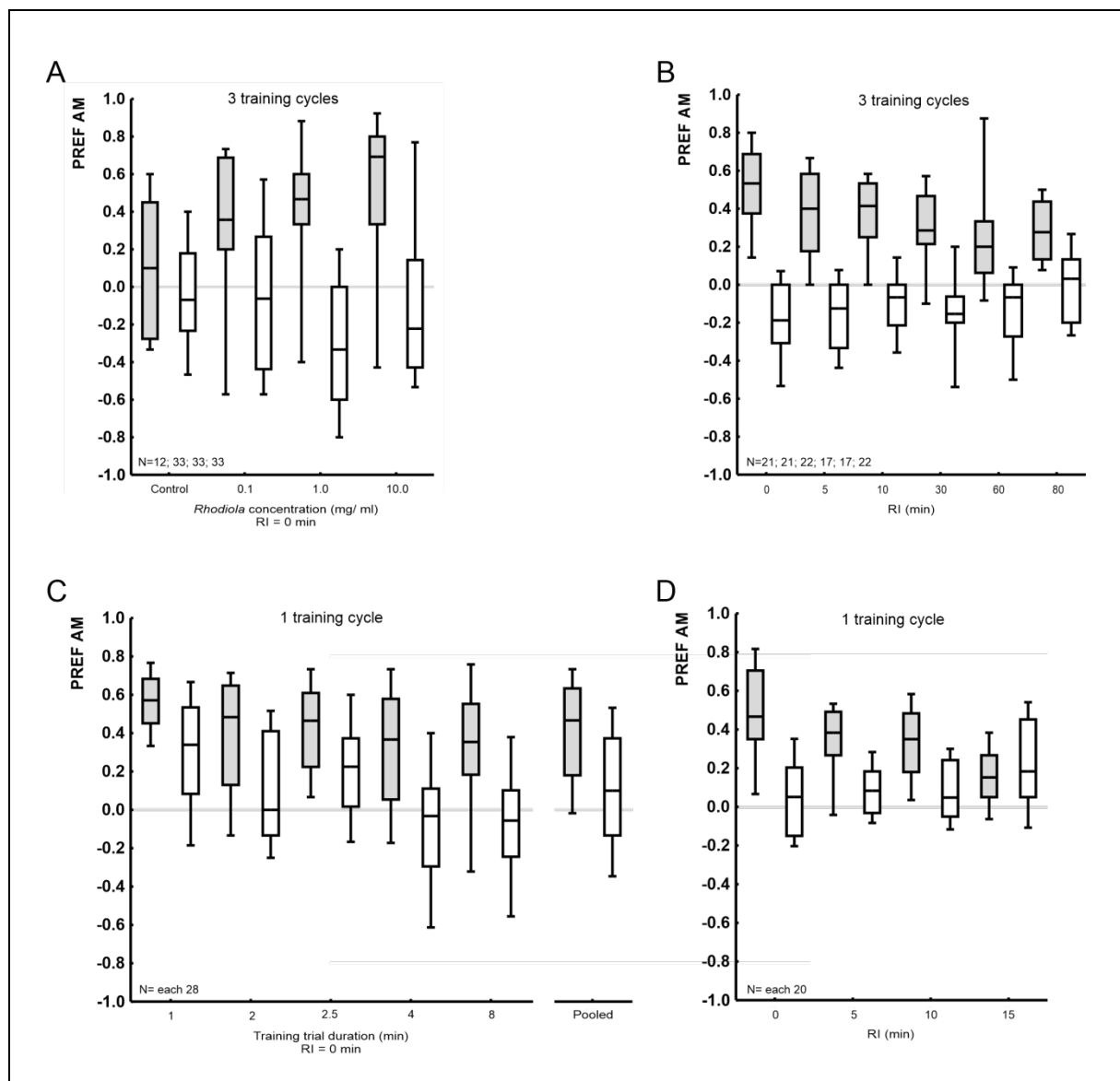


Fig. S4: Preference scores underlying the Performance Indices from Figure 1.

Visualization of the *n*-amyl acetate (AM) preference scores (PREF AM) underlying the Performance Indices from Figure 1. Preference scores after paired (grey boxes) and unpaired (white boxes) training are shown separately. The scores in A-D) correspond to Figure 1C-F. Box plots show the median as the middle line, the 25/75% quantiles as box boundaries, and the 10/90% quantiles as whiskers. Sample sizes are indicated within the figure. Data are documented in *Data file S2 Behavior data.xlsx*.

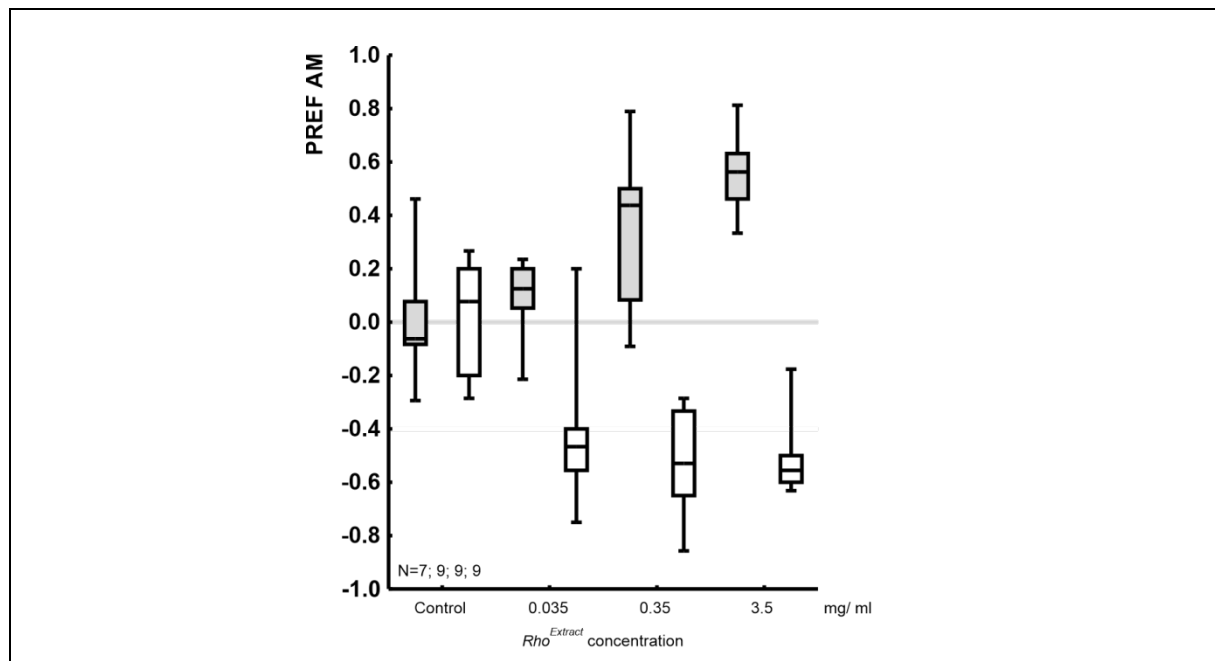


Fig. S5: Preference scores underlying the Performance Indices from Figure 2.

Visualization of the *n*-amyl acetate (AM) preference scores (PREF AM) underlying the Performance Indices from Figure 2D. Preference scores after paired (grey boxes) and unpaired (white boxes) training are shown separately. Box plots show the median as the middle line, the 25/75% quantiles as box boundaries, and the 10/90% quantiles as whiskers. Sample sizes are indicated within the figure. Data are documented in *Data file S2 Behavior data.xlsx*.

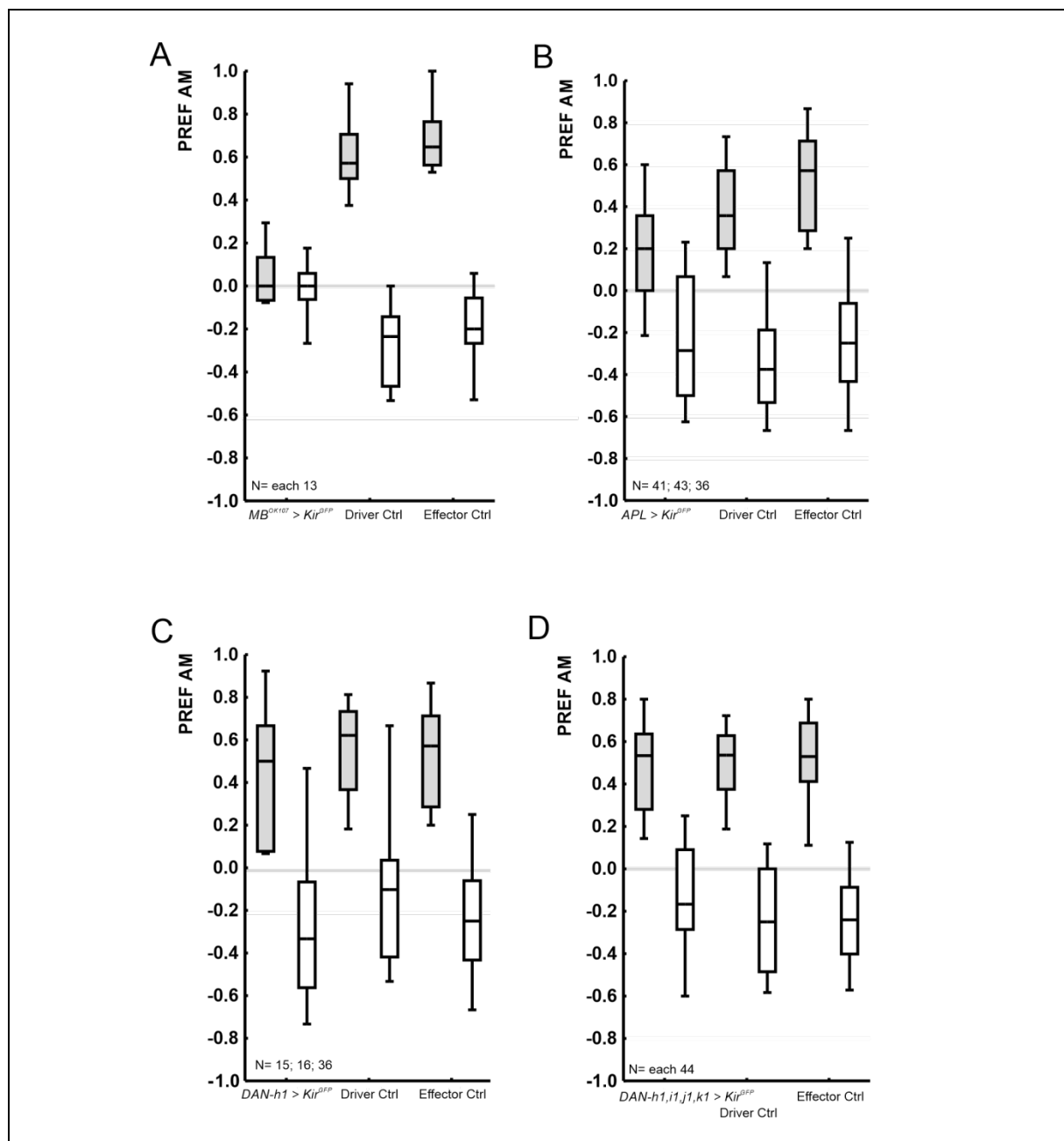


Fig. S6: Preference scores underlying the Performance Indices from Figure 3.

Visualization of the *n*-amyl acetate (AM) preference scores (Prefs AM) underlying the Performance Indices from Figure 3. Preference scores after paired (grey boxes) and unpaired (white boxes) training are shown separately. The scores in A, B, C, D) correspond to Figure 3C, E, G, I. Box plots show the median as the middle line, the 25/75% quantiles as box boundaries, and the 10/90% quantiles as whiskers. Sample sizes are indicated within the figure. Data are documented in *Data file S2 Behavior data.xlsx*.

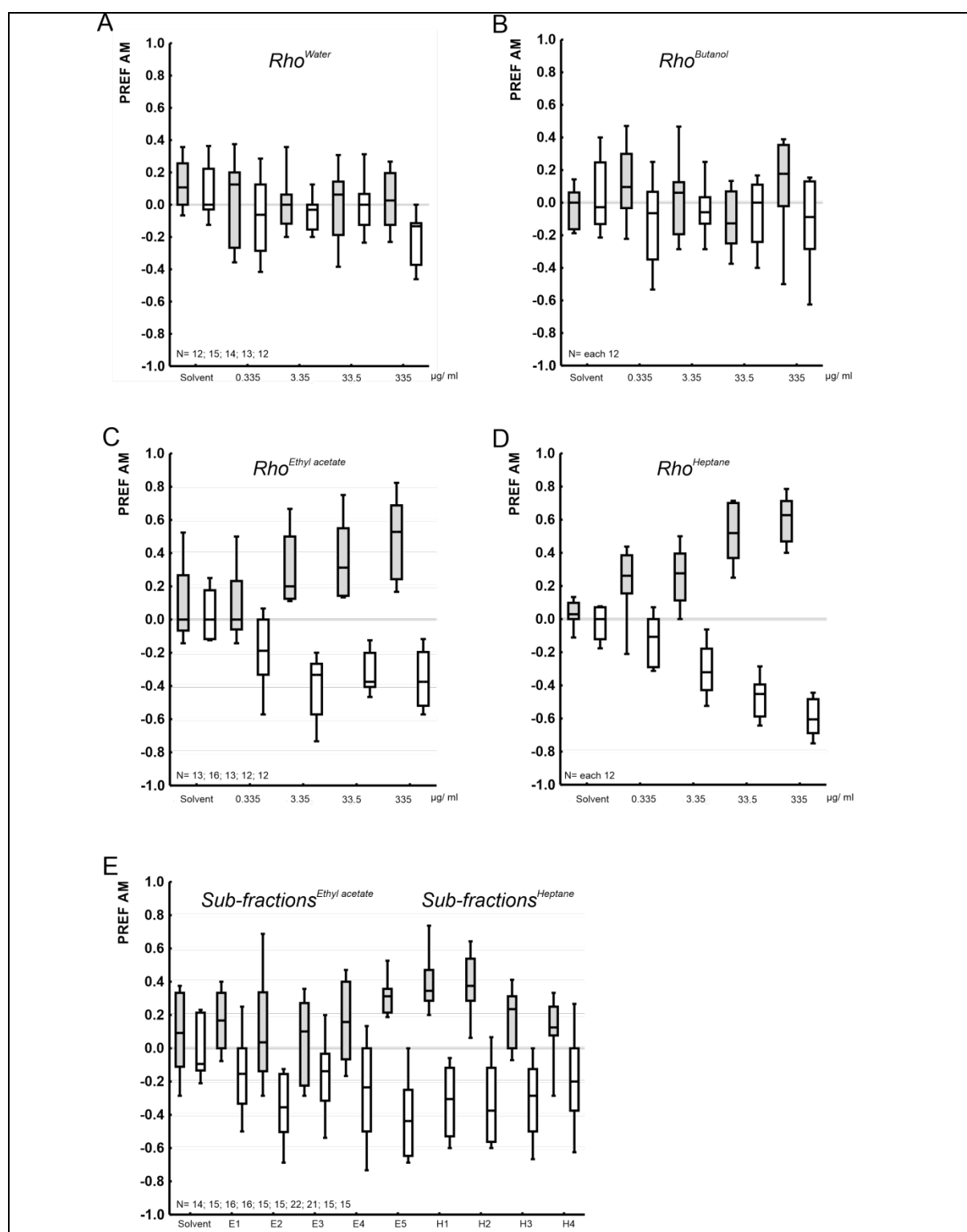


Fig. S7: Preference scores underlying the Performance Indices from Figure 4.

Visualization of the *n*-amyl acetate (AM) preference scores (PREF AM) underlying the Performance Indices from Figure 4. Preference scores after paired (grey boxes) and unpaired (white boxes) training are shown separately. The scores in A-E) correspond to Figure 4C-G. Box plots show the median as the middle line, the 25/75% quantiles as box boundaries, and the 10/90% quantiles as whiskers. Sample sizes are indicated within the figure. Data are documented in *Data file S2 Behavior data.xlsx*.

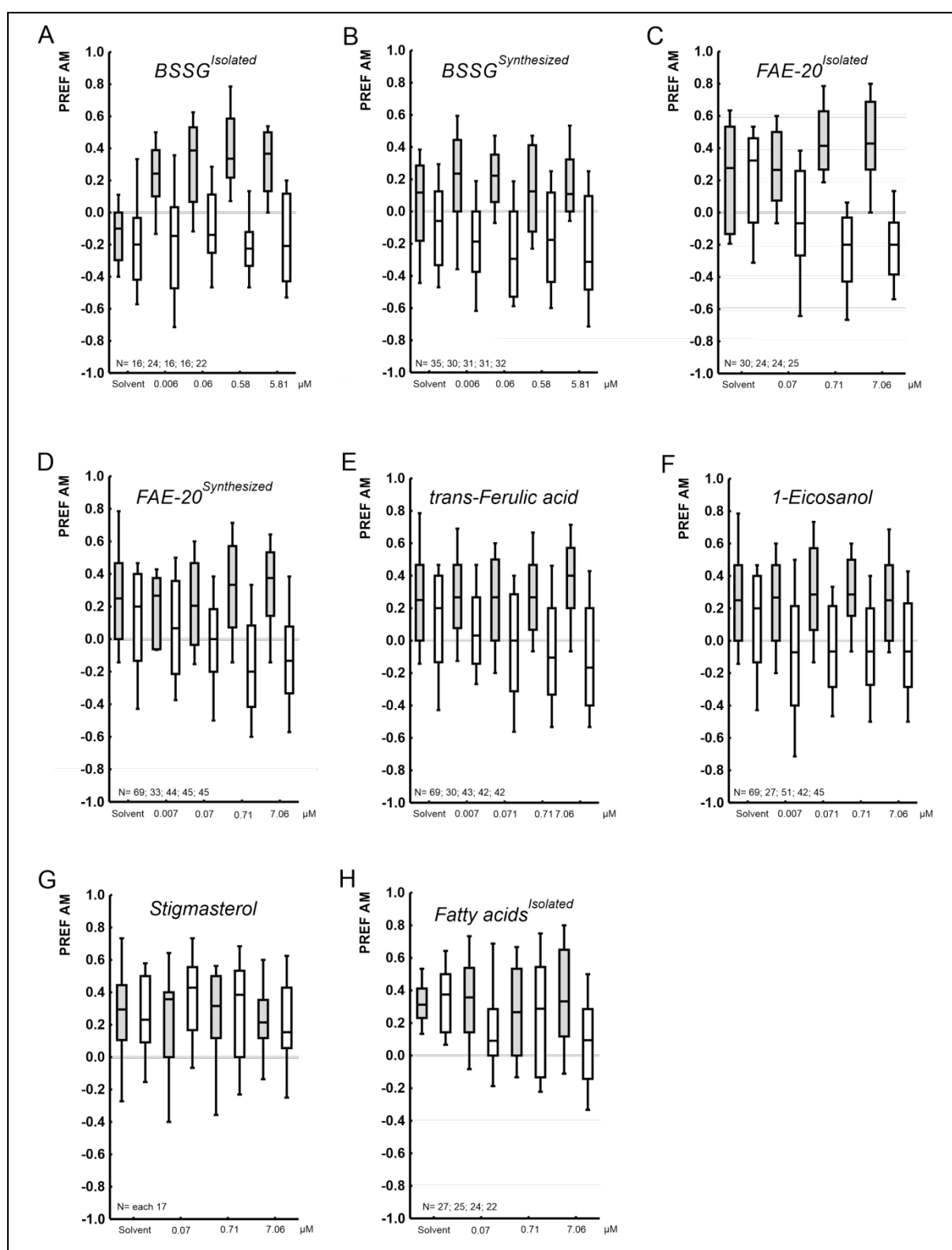


Fig. S8: Preference scores underlying the Performance Indices from Figure 5.

Visualization of the *n*-amyl acetate (AM) preference scores (PREF AM) underlying the Performance Indices from Figure 5. Preference scores after paired (grey boxes) and unpaired (white boxes) training are shown separately. The scores in A-H) correspond to Figure 5A-H. Box plots show the median as the middle line, the 25/75% quantiles as box boundaries, and the 10/90% quantiles as whiskers. Sample sizes are indicated within the figure. Data are documented in *Data file S2 Behavior data.xlsx*.

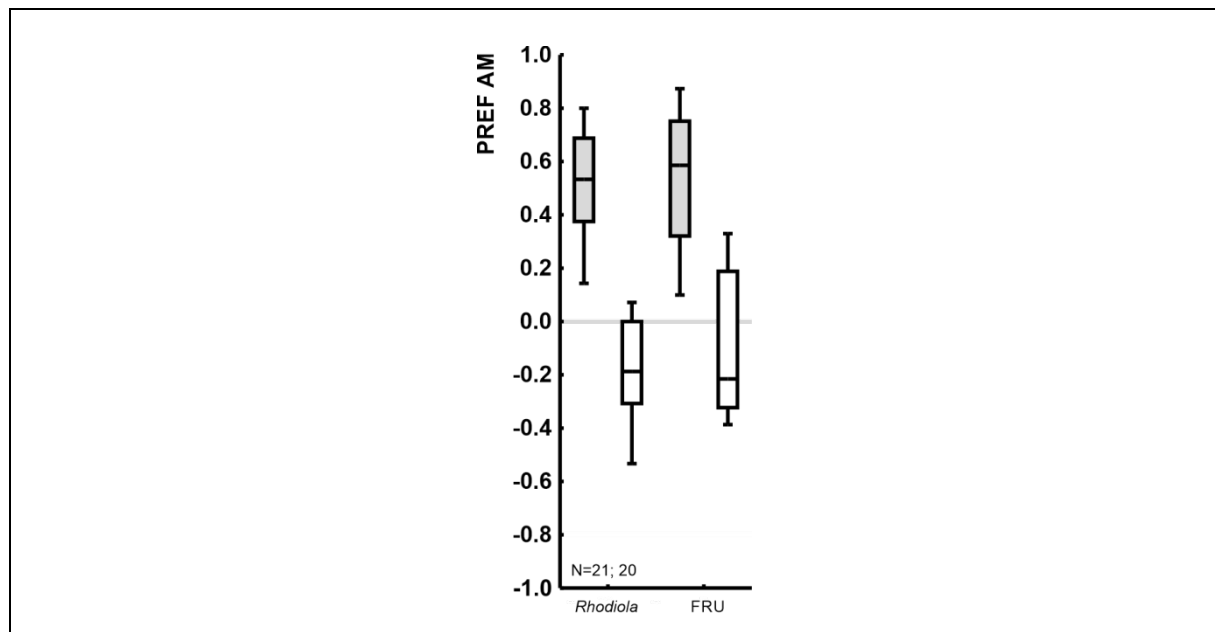


Fig. S9: Preference scores underlying the Performance Indices from Figure S1.

Visualization of the *n*-amyl acetate (AM) preference scores (PREF AM) underlying the Performance Indices from Figure S1. Preference scores after paired (grey boxes) and unpaired (white boxes) training are shown separately. Box plots show the median as the middle line, the 25/75% quantiles as box boundaries, and the 10/90% quantiles as whiskers. Sample sizes are indicated within the figure. Data are documented in *Data file S2 Behavior data.xlsx*.

Table S1. HR-ESI-MS signals (m/z features) correlating to the rewarding effect of *Rhodiola* fractions

Rank no.	FTICR-HR m/z	Spearman coefficient	Formula	MW	RDB	Calculated	Proposal
1	485.36057	0.764	C ₂₉ H ₅₀ O ₄ Na ⁺	462	4.5	485.36013	-
2	365.26635	0.664	C ₂₀ H ₃₈ O ₄ Na ⁺	342	1.5	365.26623	oxygenated fatty acid
3	497.36086	0.662	C ₃₀ H ₅₀ O ₄ Na ⁺	474	5.5	497.36013	ferulic acid eicosyl ester (FAE-20)
4	629.40341	0.624	C ₃₅ H ₅₈ O ₈ Na ⁺	606	6.5	629.40239	triterpene glycoside
5	393.29800	0.605	C ₂₂ H ₄₂ O ₄ Na ⁺	370	1.5	393.29753	oxygenated fatty acid
6	639.49637	0.605	C ₃₉ H ₆₈ O ₅ Na ⁺	616	5.5	639.49590	diglyceride
7	319.22432	0.595	C ₁₈ H ₃₂ O ₃ Na ⁺	296	2.5	319.22437	oxygenated fatty acid
8	335.21937	0.593	C ₁₈ H ₃₂ O ₄ Na ⁺	312	2.5	335.21928	oxygenated fatty acid
9	613.40841	0.588	C ₃₅ H ₅₈ O ₇ Na ⁺	590	6.5	613.40747	triterpene glycoside
10	359.14678	0.571	C ₁₈ H ₂₄ O ₆ Na ⁺	336	6.5	359.14651	-
11	345.13114	0.561	C ₁₇ H ₂₂ O ₆ Na ⁺	322	6.5	345.13086	-
12	435.17819	0.558	C ₂₄ H ₂₈ O ₆ Na ⁺	412	10.5	435.17781	-
13	144.47699	0.550	-				-
14	377.26626	0.536	C ₂₁ H ₃₈ O ₄ Na ⁺	354	2.5	377.26623	oxygenated fatty acid or monoglyceride
15	363.25069	0.530	C ₂₀ H ₃₆ O ₄ Na ⁺	340	2.5	363.25058	oxygenated fatty acid or diterpene
16	501.35597	0.525	C ₂₉ H ₅₀ O ₅ Na ⁺	478	4.5	501.35504	cholesterol derivative
17	555.36611	0.524	C ₃₂ H ₅₂ O ₆ Na ⁺	522	6.5	555.36561	triterpene acetate
18	315.15673	0.517	C ₁₇ H ₂₄ O ₄ Na ⁺	292	5.5	315.15668	sesquiterpene derivative
19	347.25551	0.517	C ₂₀ H ₃₆ O ₃ Na ⁺	324	2.5	347.25567	oxygenated fatty acid or diterpene
20	333.20380	0.511	C ₁₈ H ₃₀ O ₄ Na ⁺	310	3.5	333.20363	oxygenated fatty acid
21	393.26131	0.510	C ₂₁ H ₃₈ O ₅ Na ⁺	370	2.5	393.26114	oxygenated fatty acid or monoglyceride
22	409.25589	0.510	C ₂₁ H ₃₈ O ₆ Na ⁺	386	2.5	409.25606	monoglyceride
23	336.22327	0.507	C ₁₇ [¹³]CH ₃₂ O ₄ Na ⁺	312	2.5	336.22318	isotope peak of rank 8
24	379.24582	0.499	C ₂₀ H ₃₆ O ₅ Na ⁺	356	2.5	379.24549	oxygenated fatty acid or diterpene
25	348.25886	0.499	C ₁₉ [¹³]CH ₃₆ O ₃ Na ⁺	324	2.5	348.25960	isotope peak of rank 19
26	527.33480	0.497	C ₃₀ H ₄₈ O ₆ Na ⁺	504	6.5	527.33431	triterpene
27	317.20903	0.496	C ₁₈ H ₃₀ O ₃ Na ⁺	294	3.5	317.20871	oxygenated fatty acid
28	513.35563	0.491	C ₃₀ H ₅₀ O ₅ Na ⁺	490	5.5	513.35504	triterpene
29	615.49705	0.485	C ₃₉ H ₆₇ O ₅ ⁺ or C ₃₇ H ₆₈ O ₅ Na ⁺	614 592	6.5 3.5	615.49830 615.49589	diglyceride
30	457.29310	0.484	C ₂₆ H ₄₂ O ₅ Na ⁺	424	5.5	457.29244	pregnane derivative
31	345.24000	0.477	C ₂₀ H ₃₄ O ₃ ⁺	344	3.5	345.24002	oxygenated fatty acid or diterpene
32	413.37835	0.477	?				-
33	515.37170	0.476	C ₃₀ H ₅₂ O ₅ Na ⁺	492	4.5	515.37124	
34	378.26994	0.470	C ₂₀ [¹³]CH ₃₈ O ₄ Na ⁺	354	2.5	378.26958	isotope peak of rank 14
35	423.28708	0.465	C ₂₆ H ₄₀ O ₃ Na ⁺	400	6.5	423.28696	
36	437.26693	0.465	C ₂₆ H ₃₈ O ₄ Na ⁺	414	7.5	437.26623	
37	440.28543	0.465	C ₂₅ [¹³]CH ₄₀ O ₄ Na ⁺ or C ₂₀ H ₄₂ NO ₉ ⁺	416 422	6.5 0.5	440.28523 440.28541	isotope peak or NH ₄ -adduct

38	303.22935	0.464	C ₁₈ H ₃₂ O ₂ Na ⁺	280	2.5	303.22945	linoleic acid
39	375.12062	0.464	C ₁₈ H ₂₄ O ₆ K ⁺	336	6.5	375.12045	
40	441.37218	0.464	C ₃₀ H ₄₉ O ₂ ⁺ or C ₂₈ H ₅₀ O ₂ Na ⁺	440 418	6.5 3.5	441.37271 441.37030	-
41	469.36568	0.464	C ₂₉ H ₅₀ O ₃ Na ⁺	446	4.5	469.36521	
42	525.31925	0.464	C ₃₂ H ₄₅ O ₆ ⁺ C ₃₀ H ₄₆ O ₆ Na ⁺	524 502	10.5 7.5	525.32134	
43	529.35031	0.464	C ₃₀ H ₅₀ O ₆ Na ⁺	506	5.5	529.34996	
44	531.36736	0.464	C ₃₂ H ₅₁ O ₆ ⁺ or C ₃₀ H ₅₂ O ₆ Na ⁺	530 508	7.5 4.5	531.36801 531.36561	
45	545.34356	0.464	C ₃₀ H ₅₀ O ₇ Na ⁺	522	5.5	545.34311	
46	581.41817	0.464	C ₃₅ H ₅₈ O ₅ Na ⁺	558	6.5	581.41764	sitosterol glycoside – H ₂ O
47	597.41268	0.464	C ₃₅ H ₅₈ O ₆ Na ⁺	574	6.5	597.41256	-
48	616.49825	0.464	?				-
49	177.05445	0.464	C ₁₀ H ₉ O ₃ ⁺	176	6.5	177.05462	-
50	744.51450	0.464	?				-
51	771.54486	0.464	?				-

Table S2. Analytical data

[Click here to Download Table S2](#)

Table S3. Behavior data

[Click here to Download Table S3](#)